6

CROSS DIFFUSION EFFECTS ON THREE DIMENSIONAL CASSON FLUID FLOW

Content of this chapter is published in:

Journal of Applied Science and Engineering (Scopus) 23 (2), (2020) 319-331

CROSS DIFFUSION EFFECTS ON THREE DIMENSIONAL CASSON FLUID FLOW

Three dimensional modelling of the fluid flow problems are more realistic compared to lower dimensional studies. Thus this chapter is dedicated to extend work discussed in previous chapters to higher dimensions. This chapter deals with three dimensional MHD flow of Casson fluid past between horizontal plates. Here the considered fluid is conducting which passes through medium which has porosity.

6.1 Introduction of the problem:

In recent time, many researchers have been involved in doing research on mhd flow of various Non-Newtonian fluids due to their fascinating and noteworthy engineering focus with respect to utility and applications. It is established on the principle that particles of fluid would be structurally continuous. Casson fluid is a Pseudo plastic fluid, which means that it is Shear thinning fluid. The fluid is more viscous as compare to Newtonian fluids at low shear rates and is less viscous when shear rate is high.

Casson [102] introduced Casson fluid model for the prediction of the flow behavior of pigment-oil suspensions. Recently, Mahanta and shaw [23] discussed the 3D Casson fluid flow past linearly stretching sheet. First exact solution of MHD equations was found by J. Hartmann [52]. Nadeem et al. [126] studied three MHD Casson fluids flow in porous linearly stretching sheet.

Analytical solution of higher dimensional problems are not possible in most of the cases. In such cases concept of Homotopy is very useful as discussed in some of the recent articles [1, 26-28, 156]. Unsteady free convective MHD flow with heat and mass transfer is important in engineering and technology. Many researchers like, Kataria and Mittal [37], Freidoonimehr et al. [103] and Sheikholeslami and Bhatti [87] considered free convective flow with heat transfer problems. Radiations caused by effects of transfer of heat on fluid flow are vital in space technology, controlling of polymer processes or processes in which temperature is very high. Sheikholeslami and Shehzad [90] and Rashidi et al. [80] discussed effect of thermal radiation on MHD flow. Some of vital applications of flow containing heat and mass transfer with chemical reaction may be found in food processing, catalytic chemical reactors and polymer production. Investigations related to generation or absorption of heat by fluid flow is significant in various physical problems. Khan et

al. [72, 74] studied effects of chemical reaction on MHD problems. Shehzad et al. [118] studied of three dimension MHD flow with generation of heat and Hussain et al. [124] considered MHD flow with chemical reaction and heat absorption. Recently, Kumaran and Sandeep [22] studied parabolic flow of MHD Casson and Williamson fluids with cross diffusion whereas Sandeep et al. [106] considered kinematic viscosity model for 3D-Casson fluid flow on a surface at absolute zero. Porous media flow has many practical applications removal of heat from nuclear fuel, underground disposal of radioactive waste material, food storage, production of papers, oil exploration etc.. Some of relevant research studies are due to, Anantha et al. [56] and Sulochana et al. [9]. Khan et al. [73] on Casson fluid whereas Sheikholeslami et al. [93] have analyzed influence of external magnetic force on water based nanofluids. Nayak et al. Kataria and Mittal [36] investigated effect of radiation on Casson fluid flow.

6.2 Novelty of the chapter:

Purpose of this chapter is to investigate semi analytic solution of Dufour and Soret effects on unsteady MHD Casson fluid flow past over vertical plate embedded in porous medium in a rotating system. This study may find fire dynamics applications.

6.3 Mathematical Formulation of the Problem:

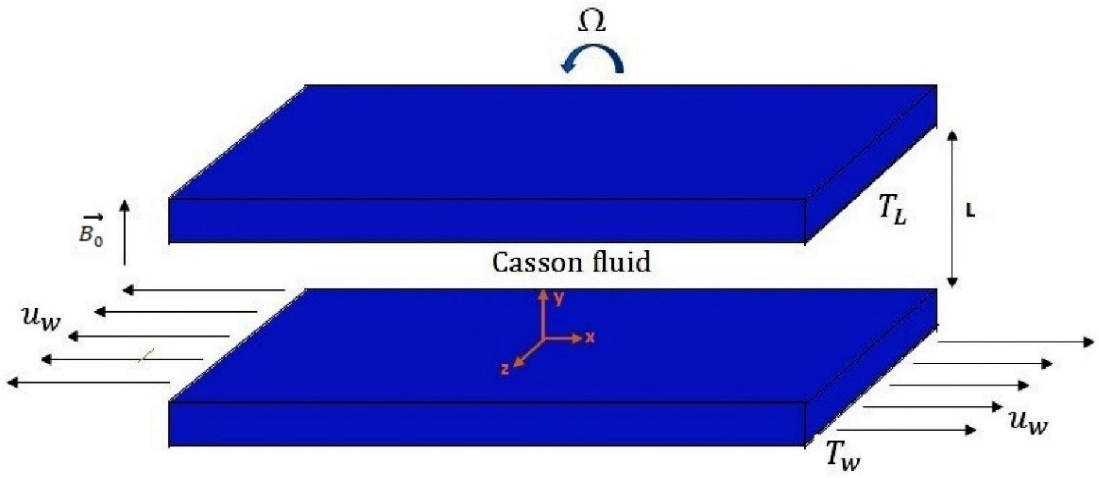

Figure 6.1 Physical sketch of the problem

It is assumed that Casson fluid flows between two horizontal parallel plates placed L units apart through a porous medium. A coordinate system (x, y, z) is such that origin is at the lower plate as shown in Figure 6.1. The lower plate is stretched by two equal forces in opposite directions. The plates along with the fluid rotate about $y-axis$ with angular velocity Ω. A uniform magnetic flux with density B_0 is applied along $y-axis$. Under these assumptions, governing equations are:

$$\frac{\partial u}{\partial x}+\frac{\partial v}{\partial y}+\frac{\partial w}{\partial z}=0 \tag{6.1}$$

$$\rho\left(u\frac{\partial u}{\partial x}+v\frac{\partial u}{\partial y}+2\Omega w\right)=\mu\left(1+\frac{1}{\gamma}\right)\left(\frac{\partial^2 u}{\partial x^2}+\frac{\partial^2 u}{\partial y^2}\right)-\sigma B^2 u-\frac{\mu\emptyset}{k_1'}u \tag{6.2}$$

$$\rho\left(v\frac{\partial v}{\partial y}\right)=\mu\left(1+\frac{1}{\gamma}\right)\left(\frac{\partial^2 v}{\partial x^2}+\frac{\partial^2 v}{\partial y^2}\right) \tag{6.3}$$

$$\rho\left(u\frac{\partial w}{\partial x}+v\frac{\partial w}{\partial y}-2\Omega w\right)=\mu\left(1+\frac{1}{\gamma}\right)\left(\frac{\partial^2 w}{\partial x^2}+\frac{\partial^2 w}{\partial y^2}\right)-\sigma B^2 w-\frac{\mu\emptyset}{k_1'}w \tag{6.4}$$

$$u\frac{\partial T}{\partial x}+v\frac{\partial T}{\partial y}+w\frac{\partial T}{\partial z}=\frac{k}{\rho c_p}\left(\frac{\partial^2 T}{\partial x^2}+\frac{\partial^2 T}{\partial y^2}+\frac{\partial^2 T}{\partial z^2}\right)+\left(\frac{D_T}{T_w}\left(\left(\frac{\partial T}{\partial x}\right)^2+\left(\frac{\partial T}{\partial y}\right)^2+\left(\frac{\partial T}{\partial z}\right)^2\right)+D_B\left(\frac{\partial C}{\partial x}\frac{\partial T}{\partial x}+\frac{\partial C}{\partial y}\frac{\partial T}{\partial y}+\frac{\partial C}{\partial z}\frac{\partial T}{\partial z}\right)\right)-\frac{\partial q_r}{\partial y}+\frac{D_T}{c_s c_p}\frac{\partial^2 C}{\partial y^2} \tag{6.5}$$

$$u\frac{\partial C}{\partial x}+v\frac{\partial C}{\partial y}+w\frac{\partial C}{\partial z}=D_B\left(\frac{\partial^2 C}{\partial x^2}+\frac{\partial^2 C}{\partial y^2}+\frac{\partial^2 C}{\partial z^2}\right)+\frac{D_T}{T_w}\left(\frac{\partial^2 T}{\partial x^2}+\frac{\partial^2 T}{\partial y^2}+\frac{\partial^2 T}{\partial z^2}\right) \tag{6.6}$$

Considering temperature difference within the flow to be sufficiently small, Using Taylor series and neglecting higher terms, q_r [127] becomes

$$q_r=-\frac{4\sigma^*}{3k^*}\frac{\partial T^4}{\partial y}=-\frac{4\sigma^*}{3k^*}\frac{\partial(4T_0{}^3T-3T_0{}^4)}{\partial y} \tag{6.7}$$

Subject to boundary conditions

$$u=ax;\ v=0;\ w=0;\ T=T_w\ at\ y=0$$

$$u=0;\ v=0;\ w=0;\ T=T_L\ at\ y=L \tag{6.8}$$

Introducing non dimensional variables

$$\eta=\frac{y}{L},\ u=axf'(\eta), v=-ahf(\eta),\ w=axg(\eta),\ \theta(\eta)=\frac{\mathrm{T}-T_L}{T_w-T_L},\ \mathrm{C}(\eta)=\frac{\mathrm{C}-C_L}{C_w-C_L} \tag{6.9}$$

Therefore, the governing momentum and energy equations for this problem are given in dimensionless form by:

$$\left(1+\frac{1}{\gamma}\right)f^{iv}-Re(f'f''-ff''')-2R_k g'-\left(M^2+\frac{1}{k_1}\right)f''=0 \tag{6.10}$$

$$\left(1+\frac{1}{\gamma}\right)g''-Re(f'g-fg')+2R_k f'-\left(M^2+\frac{1}{k_1}\right)g=0 \tag{6.11}$$

$$(1+\mathrm{R})\theta'' + PrRe\, f\theta' + NbC'\theta' + Nt\theta'^2 + Df\, C'' = 0 \quad (6.12)$$

$$NbC'' + Nt\theta'' + Nb\, Re\, Sc\, fC' = 0 \quad (6.13)$$

Subject to

$$f = 0, f' = 1, g = 0, \theta = 1,\ C = 1\ at\ \eta = 0$$

$$f = 0, f' = 0, g = 0, \theta = 0,\ C = 0\ at\ \eta = 1 \quad (6.14)$$

Where

$$Pr = \frac{\mu\, c_p}{k}, \qquad Sc = \frac{\mu}{\rho D_B}, \qquad M^2 = \frac{\sigma {B_0}^2 L^2}{\rho\nu}, \qquad \frac{1}{k} = \frac{\nu\emptyset^2}{k_1\nu}, \qquad K_O = \frac{\Omega L^2}{\nu},$$

$$Re = \frac{aL^2}{\nu}, \alpha = \frac{k}{\rho c_p}, Nb = \frac{D_B C_L}{\alpha}$$

6.4 Solution of the Problem:

To solve equations (6.10) – (6.13) subject to boundary conditions (6.14), HAM [122] is employed.

Initial guess is:

$$f_0(\eta) = \frac{-2}{e^2-4e+3} + \frac{e-1}{e-3}\eta + \frac{2-e}{e^2-4e+3}e^{\eta} + \frac{e}{e^2-4e+3}e^{-\eta};\ g_0(\eta) = 0;\ \theta_0(\eta) = 1-\eta;$$

$$C_0(\eta) = 1-\eta; \quad (6.15)$$

with auxiliary linear operators:

$$L_f = \frac{\partial^4 f}{\partial\eta^4} - \frac{\partial^2 f}{\partial\eta^2},\ L_g = \frac{\partial^2 g}{\partial\eta^2} - g,\ L_\theta = \frac{\partial^2\theta}{\partial\eta^2},\ L_{\mathrm{C}} = \frac{\partial^2 \mathrm{C}}{\partial\eta^2} \quad (6.16)$$

Satisfying

$$L_f(C_1 + C_2\,\eta + C_3 e^{\eta} + C_4 e^{-\eta}) = 0,\ L_g(C_5 e^{\eta} + C_6 e^{-\eta}) = 0,\ L_\theta(C_7 + C_8\eta) = 0,$$

$$L_C(C_9 + C_{10}\eta) = 0. \quad (6.17)$$

where $c_1,\ c_2, \ldots, c_{10}$ are the arbitrary constants.

The zeroth order deformation problems are constructed as follows:

$$(1-p)L_f\left[\hat{f}(\eta;\ p) - f_0(\eta)\right] = p\hbar_f N_f\left[\hat{f}(\eta;\ p), \hat{g}(\eta;\ p), \hat{\theta}(\eta;\ p), \hat{C}(\eta;\ p)\right] \quad (6.18)$$

$$(1-p)L_g[\hat{g}(\eta;\ p) - g_0(\eta)] = p\hbar_g N_g\left[\hat{f}(\eta;\ p), \hat{g}(\eta;\ p), \hat{\theta}(\eta;\ p), \hat{C}(\eta;\ p)\right] \quad (6.19)$$

$$(1-p)L_\theta\left[\hat{\theta}(\eta;\ p) - \theta_0(\eta)\right] = p\hbar_\theta N_\theta\left[\hat{f}(\eta;\ p), \hat{g}(\eta;\ p), \hat{\theta}(\eta;\ p), \hat{C}(\eta;\ p)\right] \quad (6.20)$$

$$(1-p)L_C\left[\hat{C}(\eta;\ p) - C_0(\eta)\right] = p\hbar_C N_C\left[\hat{f}(\eta;\ p), \hat{g}(\eta;\ p), \hat{\theta}(\eta;\ p), \hat{C}(\eta;\ p)\right] \quad (6.21)$$

Subject to the boundary conditions:

$$\hat{f}(0;\ p) = 0, \quad \hat{f}'(0;\ p) = 1; \tag{6.22}$$

$$\hat{f}(1;\ p) = 0, \quad \hat{f}'(1;\ p) = 0; \tag{6.23}$$

$$\hat{g}(0;\ p) = 0, \quad \hat{g}(1;\ p) = 0; \tag{6.24}$$

$$\hat{\theta}(0;\ p) = 1, \quad \hat{\theta}(1;\ p) = 0, \tag{6.25}$$

$$\hat{C}(0;\ p) = 1, \quad \hat{C}(1;\ p) = 0, \tag{6.26}$$

The nonlinear operators are defined as

$$N_f\left[\hat{f}(\eta;\ p), \hat{g}(\eta;\ p), \hat{\theta}(\eta;\ p), \hat{C}(\eta;\ p)\right] = \left(1 + \frac{1}{\gamma}\right)\frac{\partial^4 \hat{f}}{\partial \eta^4} - Re\left(\frac{\partial \hat{f}}{\partial \eta}\frac{\partial^2 \hat{f}}{\partial \eta^2} - \hat{f}\frac{\partial^3 \hat{f}}{\partial \eta^3}\right) - 2R_k\ \frac{\partial \hat{g}}{\partial \eta} - \left(M^2 + \frac{1}{k_1}\right)\frac{\partial^2 \hat{f}}{\partial \eta^2} \tag{6.27}$$

$$N_g\left[\hat{f}(\eta;\ p), \hat{g}(\eta;\ p), \hat{\theta}(\eta;\ p), \hat{C}(\eta;\ p)\right] = \left(1 + \frac{1}{\gamma}\right)\frac{\partial^2 \hat{g}}{\partial \eta^2} - Re\left(\hat{g}\ \frac{\partial \hat{f}}{\partial \eta} - \hat{f}\ \frac{\partial \hat{g}}{\partial \eta}\right) + 2R_k\ \frac{\partial \hat{f}}{\partial \eta} - \left(M^2 + \frac{1}{k_1}\right)\hat{g} \tag{6.28}$$

$$N_\theta\left[\hat{f}(\eta;\ p), \hat{g}(\eta;\ p), \hat{\theta}(\eta;\ p), \hat{C}(\eta;\ p)\right] = 1 + R\frac{\partial^2 \hat{\theta}}{\partial \eta^2} + PrRe\ \hat{f}\frac{\partial \hat{\theta}}{\partial \eta} + Nb\frac{\partial \hat{C}}{\partial \eta}\frac{\partial \hat{\theta}}{\partial \eta} + Nt\left(\frac{\partial \hat{\theta}}{\partial \eta}\right)^2 + D_f\frac{\partial^2 \hat{C}}{\partial \eta^2} \tag{6.29}$$

$$N_C\left[\hat{f}(\eta;\ p), \hat{g}(\eta;\ p), \hat{\theta}(\eta;\ p), \hat{C}(\eta;\ p)\right] = Nb\frac{\partial^2 \hat{\mathbb{C}}}{\partial \eta^2} + Nt\frac{\partial^2 \hat{\theta}}{\partial \eta^2} + NbReSc\hat{f}\frac{\partial \hat{\mathbb{C}}}{\partial \eta} \tag{6.30}$$

Where $\hat{f}(\eta;\ p), \hat{g}(\eta;\ p), \hat{\theta}(\eta;\ p)$ and $\hat{C}(\eta;\ p)$ are unknown functions with respect to η and p. $\hbar_f, \hbar_g, \hbar_\theta$ and $\hbar_C$ are the non-zero auxiliary parameters and N_f, N_g, N_θ and N_C are the nonlinear operators.

Also $p \in (0,\ 1)$ is an embedding parameter. For $p = 0$ and $p = 1$ we have

$$\hat{f}(\eta; 0) = f_0(\eta),\ \hat{f}(\eta; 1) = f(\eta), \tag{6.31}$$

$$\hat{g}(\eta; 0) = g_0(\eta),\ \hat{g}(\eta; 1) = g(\eta), \tag{6.32}$$

$$\hat{\theta}(\eta; 0) = \theta_0(\eta),\ \hat{\theta}(\eta; 1) = \theta(\eta), \tag{6.33}$$

$$\hat{C}(\eta; 0) = C_0(\eta),\ \hat{C}(\eta; 1) = C(\eta) \tag{6.34}$$

Taylor's series expansion results in:

$$\hat{f}(\eta;\ p) = f_0(\eta) + \sum_{m=1}^{\infty} f_m(\eta)p^m, \tag{6.35}$$

$$\hat{g}(\eta;\ p) = g_0(\eta) + \sum_{m=1}^{\infty} g_m(\eta)p^m, \quad (6.36)$$

$$\hat{\theta}(\eta;\ p) = \theta_0(\eta) + \sum_{m=1}^{\infty} \theta_m(\eta)p^m, \quad (6.37)$$

$$\hat{C}(\eta;\ p) = C_0(\eta) + \sum_{m=1}^{\infty} C_m(\eta)p^m, \quad (6.38)$$

Where

$$f_m(\eta) = \frac{1}{m!}\left[\frac{\partial^m f(\eta;\ p)}{\partial p^m}\right]_{p=0}, \quad (6.39)$$

$$g_m(\eta) = \frac{1}{m!}\left[\frac{\partial^m g(\eta;\ p)}{\partial p^m}\right]_{p=0}, \quad (6.40)$$

$$\theta_m(\eta) = \frac{1}{m!}\left[\frac{\partial^m \theta(\eta;\ p)}{\partial p^m}\right]_{p=0}, \quad (6.41)$$

$$C_m(\eta) = \frac{1}{m!}\left[\frac{\partial^m \Phi(\eta;\ p)}{\partial p^m}\right]_{p=0}, \quad (6.42)$$

It should be noted that the convergence in the above series strongly depends upon $\hbar_f, \hbar_g, \hbar_\theta$ and $\hbar_C$. Assuming that these nonzero auxiliary parameters are chosen so that Equations (6.18)–(6.21) converges at $p = 1$, hence one can obtain the following:

$$f(\eta) = f_0(\eta) + \sum_{m=1}^{\infty} f_m(\eta), \quad (6.43)$$

$$g(\eta) = g_0(\eta) + \sum_{m=1}^{\infty} g_m(\eta), \quad (6.44)$$

$$\theta(\eta) = \theta_0(\eta) + \sum_{m=1}^{\infty} \theta_m(\eta), \quad (6.45)$$

$$C(\eta) = C_0(\eta) + \sum_{m=1}^{\infty} C_m(\eta), \quad (6.46)$$

Differentiating the zeroth order deformation (6.18) – (6.21) and (6.22) – (6.26) m times with respect to p and substituting $p = 0$, and finally dividing by $m!$, we obtain the m[th] order deformation ($m \geq 1$).

$$L_f[f_m(\eta) - \chi_m f_{m-1}(\eta)] = \hbar_f R_{f,m}(\eta), \quad (6.47)$$

$$L_g[g_m(\eta) - \chi_m g_{m-1}(\eta)] = \hbar_g R_{g,m}(\eta), \quad (6.48)$$

$$L_\theta[\theta_m(\eta) - \chi_m \theta_{m-1}(\eta)] = \hbar_\theta R_{\theta,m}(\eta), \quad (6.49)$$

$$L_C[C_m(\eta) - \chi_m C_{m-1}(\eta)] = \hbar_C R_{C,m}(\eta), \quad (6.50)$$

Subject to the boundary conditions

$$f_m(0) = f_m'(0) = 0, \quad (6.51)$$

$$f_m(1) = f_m'(1) = 0, \quad (6.52)$$

$$g_m(0) = g_m(1) = 0, \quad (6.53)$$

$$\theta_m(0) = \theta_m(1) = 0, \quad (6.54)$$

$$C_m(0) = C_m(1) = 0, \quad (6.55)$$

with

$$R_{f,m}(\eta) = \left(1+\frac{1}{\gamma}\right) f_{m-1}^{iv} - Re\left(\sum_{j=0}^{m-1} f_j' f_{m-1-j}'' - \sum_{j=0}^{m-1} f_j f_{m-1-j}'''\right) - 2Krg_{m-1}' - \left(M^2+\frac{1}{k_1}\right) f_{m-1}'' \quad (6.56)$$

$$R_{g,m}(\eta) = \left(1+\frac{1}{\gamma}\right) g_{m-1}'' - Re\left(\sum_{j=0}^{m-1} f_j' g_{m-1-j} - \sum_{j=0}^{m-1} f_j g_{m-1-j}'\right) + 2Krf_{m-1}' - \left(M^2+\frac{1}{k_1}\right) g_{m-1} \quad (6.57)$$

$$R_{\theta,m}(\eta) = \theta_{m-1}'' + Pr\, Re\, a_2 \sum_{j=0}^{m-1} f_j \theta_{m-1-j}' + Nb \sum_{j=0}^{m-1} C_j' \theta_{m-1-j}' + Nt \sum_{j=0}^{m-1} \left(\theta_j' \theta_{m-1-j}' + D_f C''_{m-1}\right) \quad (6.58)$$

$$R_{C,m}(\eta) = NbC_{m-1}'' + Nt\theta_{m-1}'' + NbReSc \sum_{j=0}^{m-1} f_j C_{m-1-j}' \quad (6.59)$$

$$\text{with } \chi_m = \begin{cases} 0, & m \le 1 \\ 1, & m \ge 1 \end{cases}, \quad (6.60)$$

Solving the corresponding mth-order deformation equations,

$$f_m(\eta) = f_m^*(\eta) + C_1 + C_2\,\eta + C_3 e^{\eta} + C_4 e^{-\eta} \quad (6.61)$$

$$g_m(\eta) = g_m^*(\eta) + C_5 e^{-\eta} + C_6 e^{\eta} \quad (6.62)$$

$$\theta_m(\eta) = \theta_m^*(\eta) + C_7 + C_8\eta \quad (6.63)$$

$$C_m(\eta) = C_m^*(\eta) + C_9 + C_{10}\eta \quad (6.64)$$

Here f_m^*, g_m^*, θ_m^* *and* C_m^* are given by are particular solutions of the corresponding mth-order equations and the constants $C_i (\, i = 1,2, \ldots,6)$ are to be determined by the boundary conditions.

6.4.1 Convergence Analysis:

Convergence of the HAM solutions and their rate of approximations strongly depend on the values of the auxiliary parameters $\hbar_f, \hbar_g, \hbar_\theta$ and $\hbar_C$. For this persistence, the associated h-curves are plotted in Figure 6.2 and Figure 6.3, where Figure 6.2 shows h-curves for *f, g* and θ and Figure 6.3 displays h-curve for C. Acceptable choices for the auxiliary parameters are obtained.

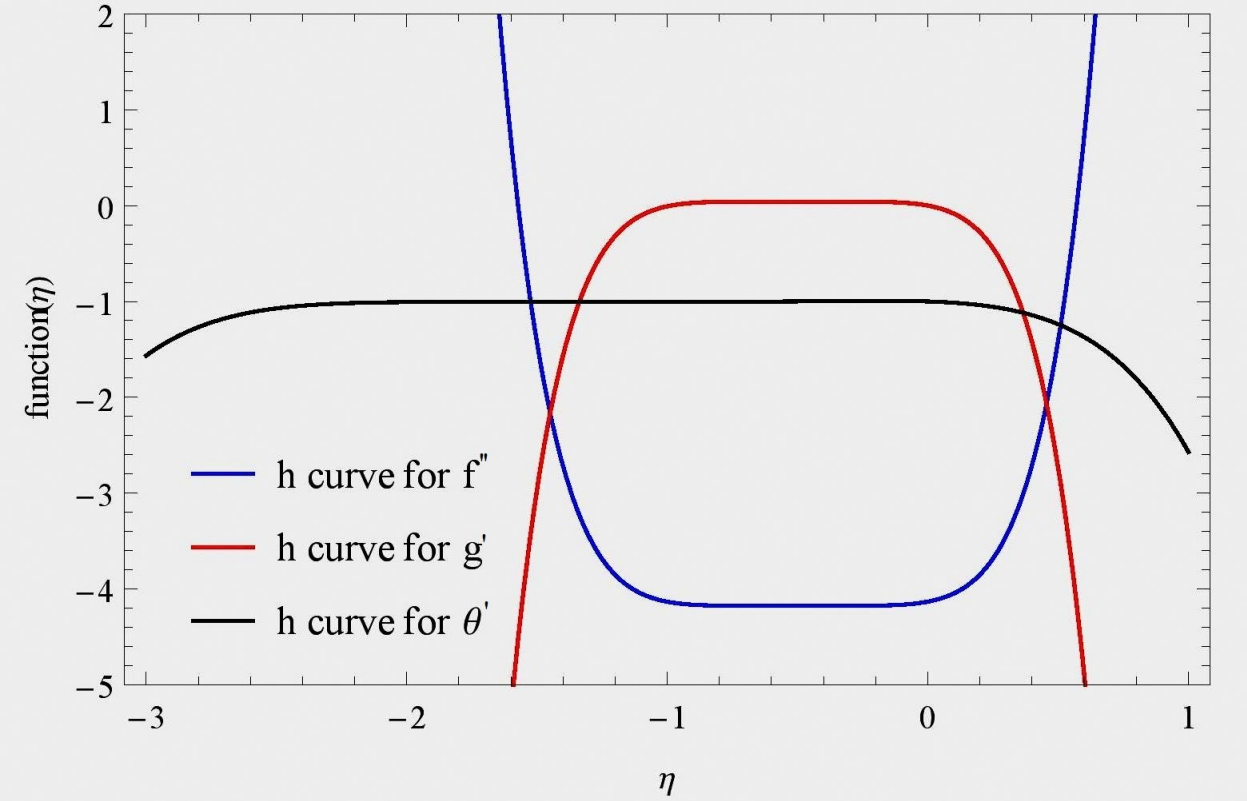

Figure 6.2: h-curve of $f''(\eta), g'(\eta)$and $\theta'(\eta)$

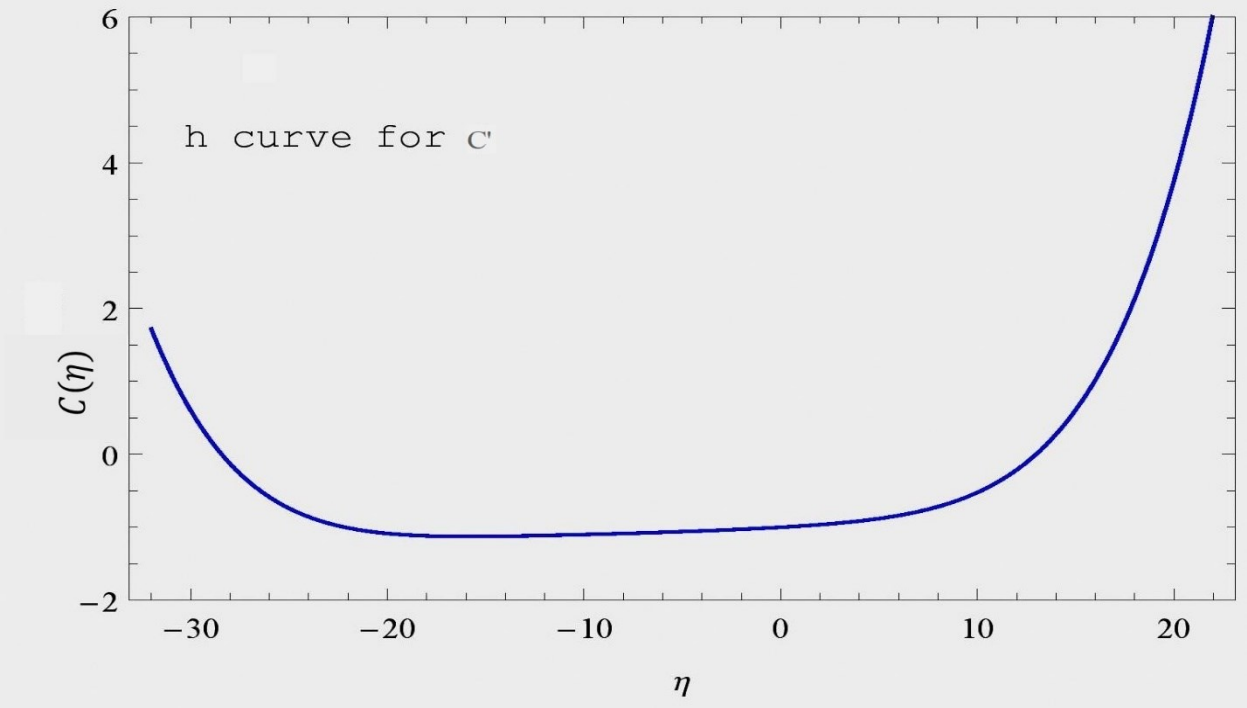

Figure 6.3: h-curve of $C'(\eta)$

6.5 Results and Discussion:

The physics of the problem through various graphs of velocity, temperature and concentration profiles are displayed in this section. Solutions for different parameters are plotted using Mathematica. Effects of different parameters: Magnetic parameter, Reynolds number, Radiation parameter, Rotation parameter, nanoparticle volume fraction, Permeability parameter, Prandtl number, Thermophoretic parameter, Brownian parameter and Schmidt Number on fluid flow is represented through Figures 4 - 32.

Figures 4 – 6 indicate effect of magnetic field M on velocity profiles. We can see here that increment in M leads to decrement in velocity. The reason of this is the Lorentz force induced on fluid. We can see the effect of Casson fluid parameter γ on velocity profiles from Figures 7 – 9. When we raise the value of γ velocity will also increase. Figures 10 – 12 reveal effects of k_1 on fluid velocity. It is clear from the figures that, permeability parameter k_1 tends to improve velocity. As k_1 increases, the wholes becomes bigger which allows more fluid to flow, hence velocity increases. Figures 13 – 15 displays negative impact of rotating parameter R_k on velocity in x and y direction whereas positive impact in z direction. Physically this is true due to the effects of Coriolis force.

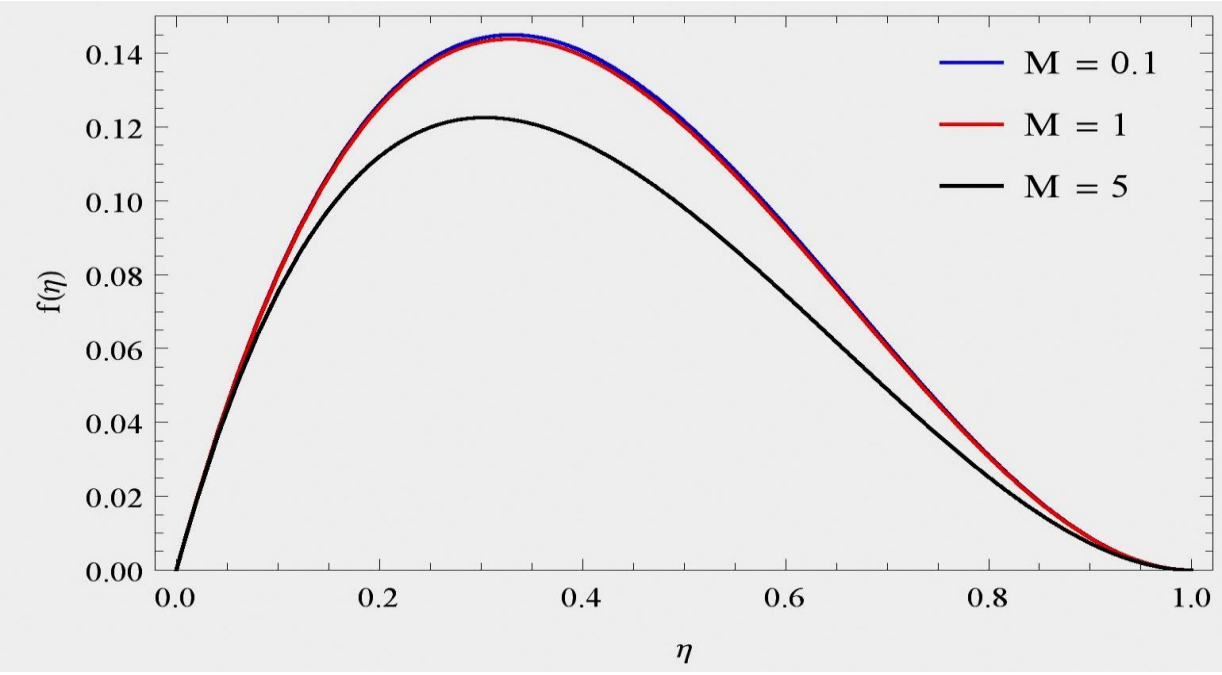

Figure 6.4: $f(\eta)$ for M at $\gamma = 1, k_1 = 0.5, R_k = 0.5, Pr = 10, Re = 1, Nt = 0.1, Nb = 0.1, Sc = 0.22, Df = 1$ and $R = 5$.

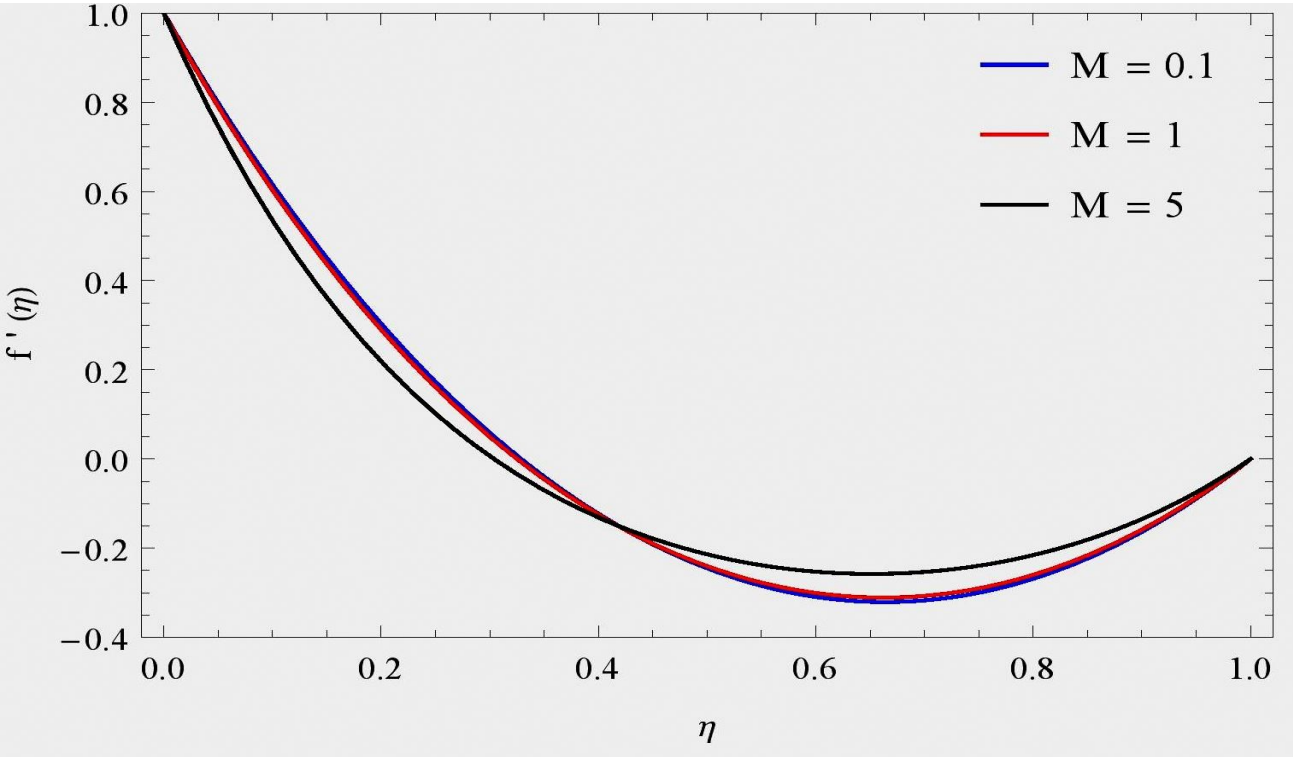

Figure 6.5: $f'(\eta)$ for M at $\gamma = 1, k_1 = 0.5, R_k = 0.5, Pr = 10, Re = 1, Nt = 0.1,$ $Nb = 0.1, Sc = 0.22, Df = 1 \; and \; R = 5.$

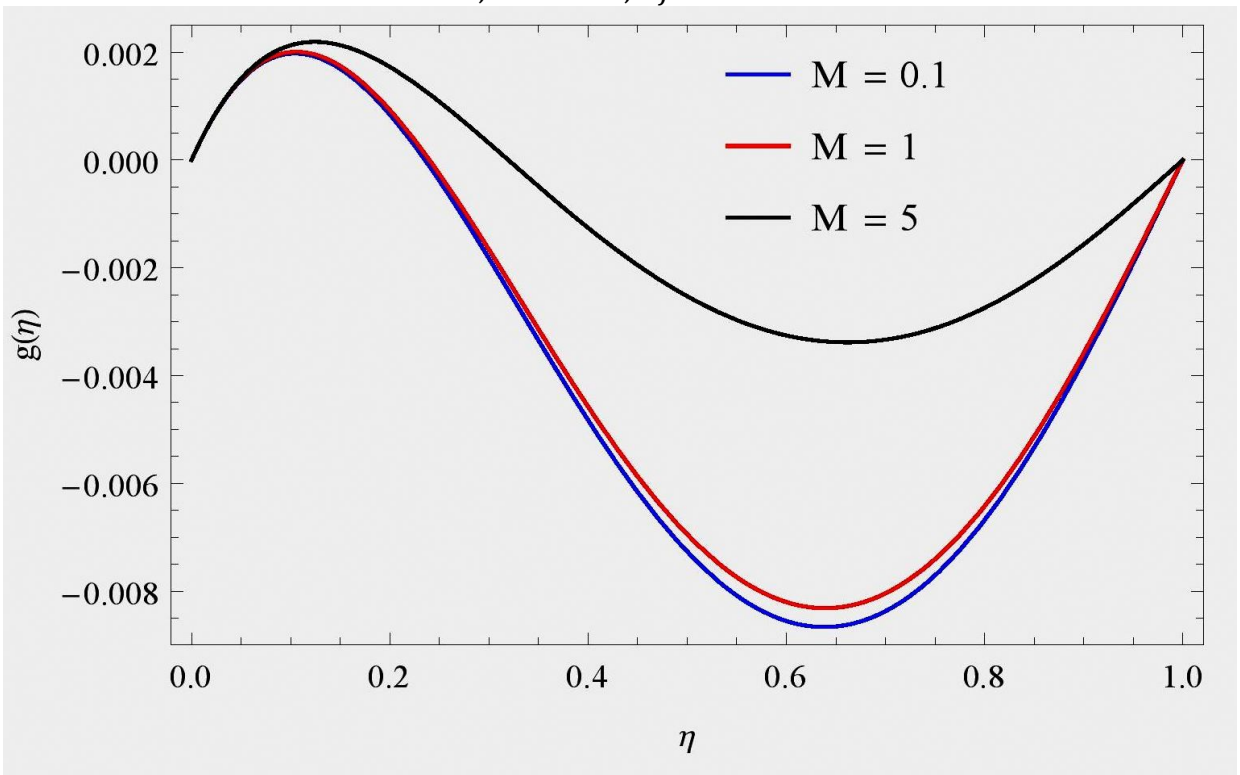

Figure 6.6: $g(\eta)$ for M at $\gamma = 1, k_1 = 0.5, R_k = 0.5, Pr = 10, Re = 1, Nt = 0.1, Nb = 0.1,$ $Sc = 0.22, Df = 1 \; and \; R = 5.$

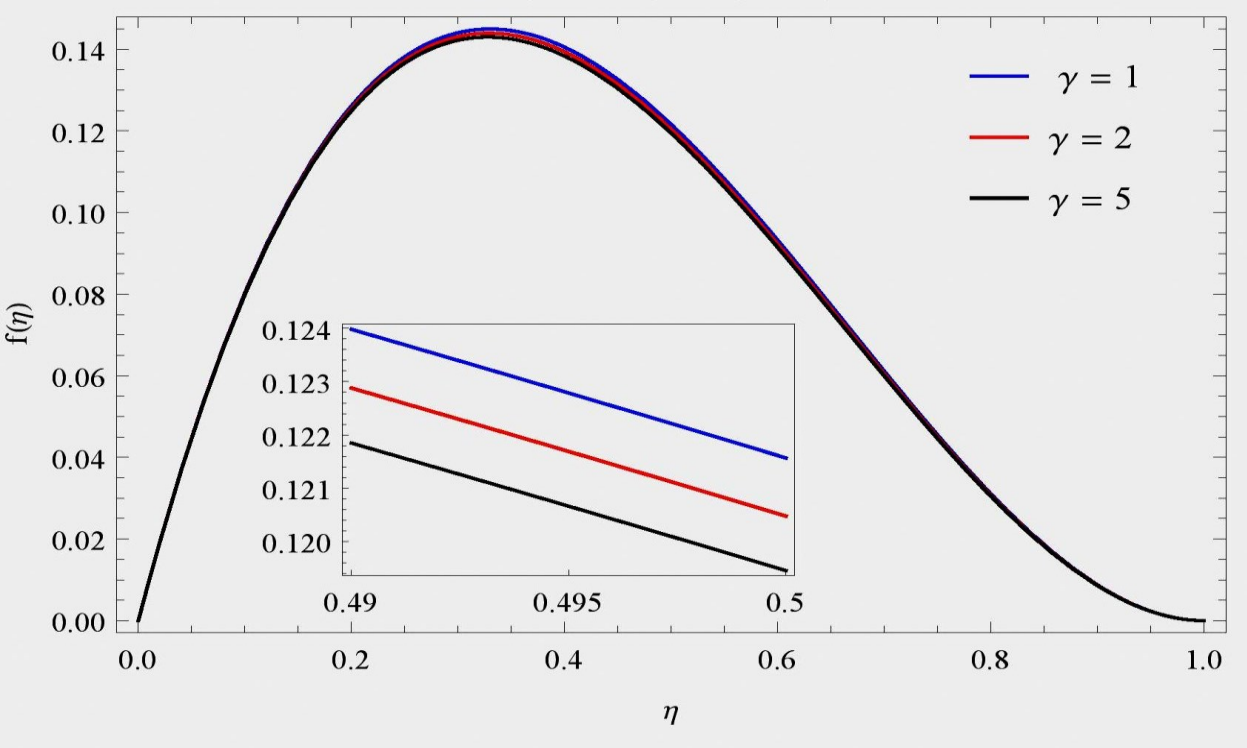

Figure 6.7: $f(\eta)$ for γ at $M = 0.1, k_1 = 0.5, R_k = 0.5, Pr = 10, Re = 1, Nt = 0.1, Nb = 0.1, Sc = 0.22, Df = 1$ *and* $R = 5$.

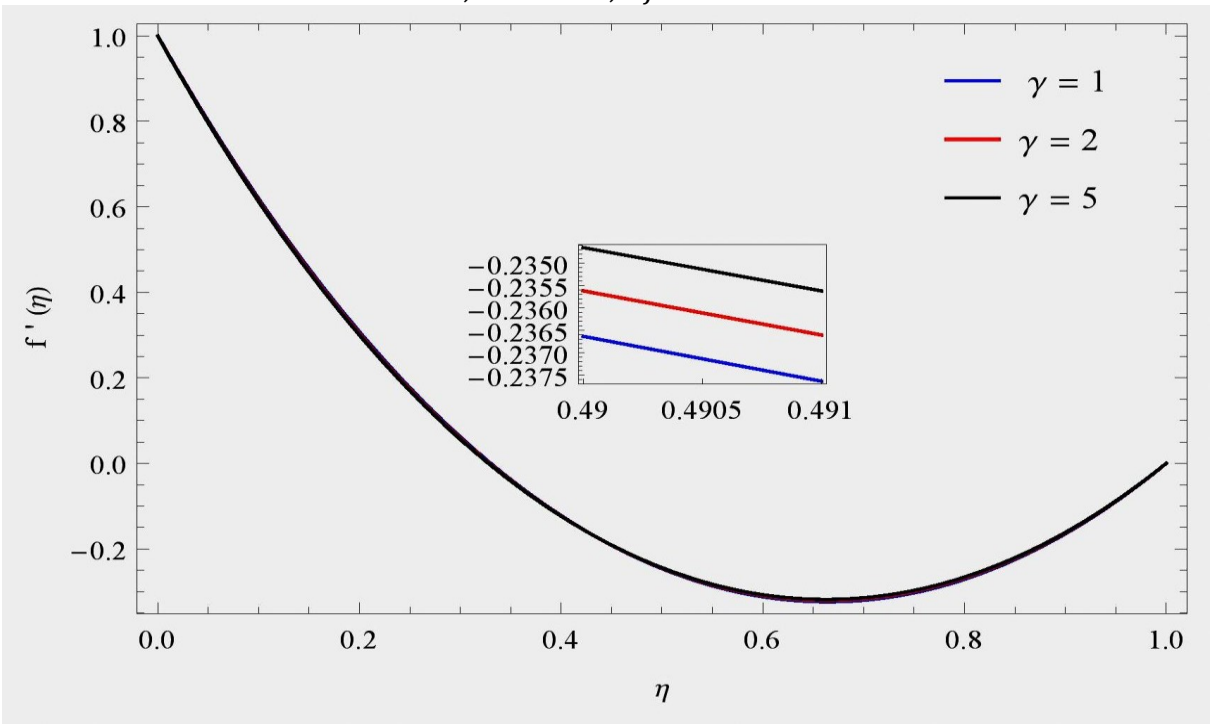

Figure 6.8: $f'(\eta)$ for γ at $M = 0.1, k_1 = 0.5, R_k = 0.5, Pr = 10, Re = 1, Nt = 0.1, Nb = 0.1, Sc = 0.22, Df = 1$ *and* $R = 5$.

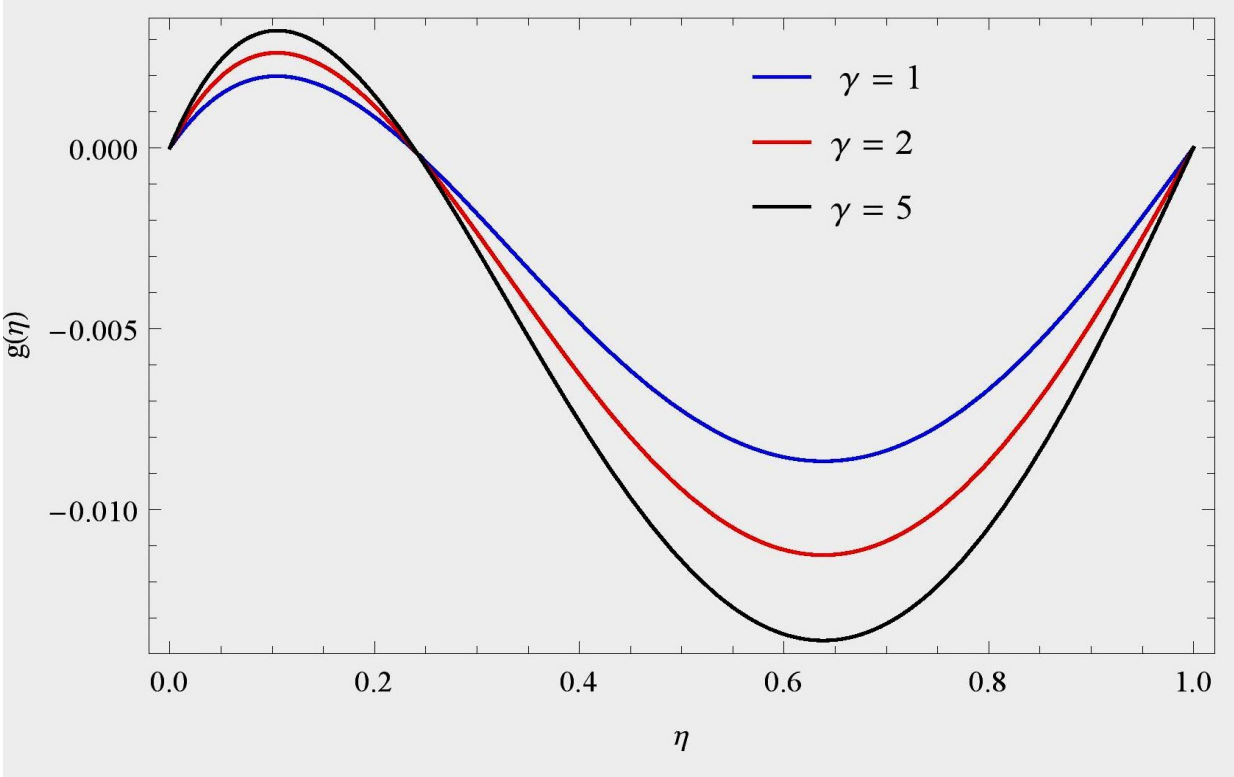

Figure 6.9: $g(\eta)$ for γ at $M = 0.1, k_1 = 0.5, R_k = 0.5, Pr = 10, Re = 1, Nt = 0.1, Nb = 0.1, Sc = 0.22, Df = 1$ *and* $R = 5$.

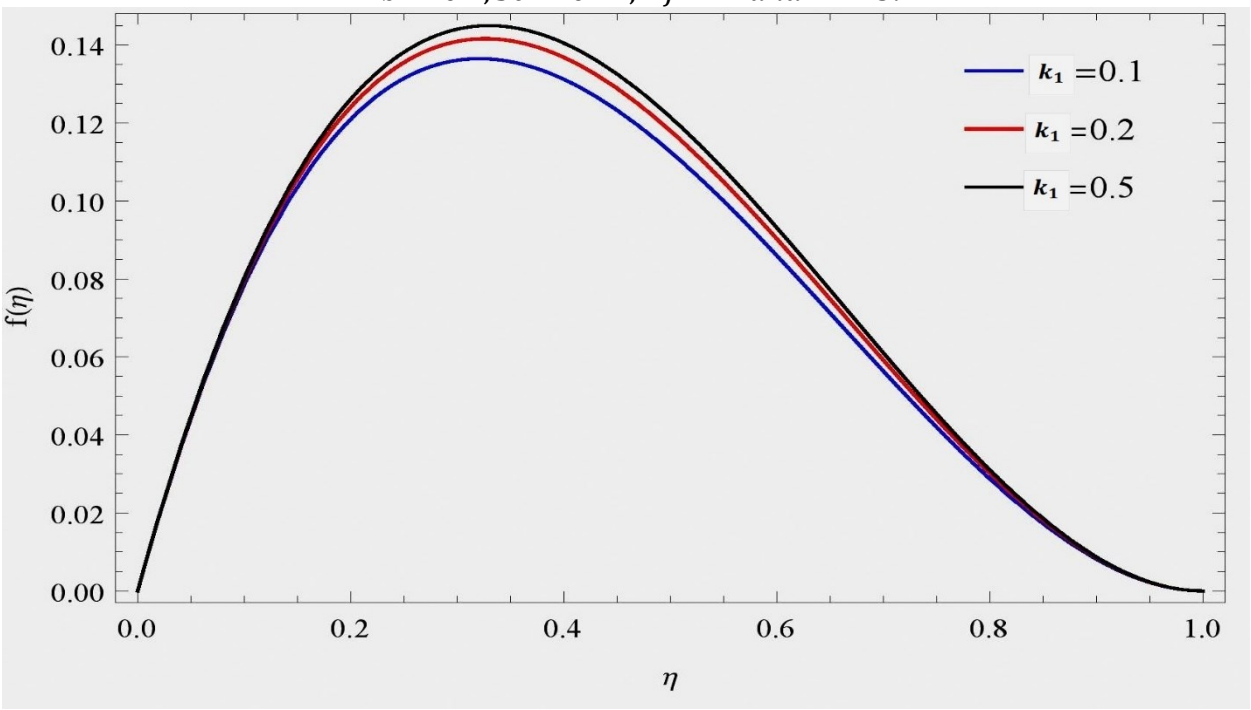

Figure 6.10: $f(\eta)$ for k_1 at $\gamma = 1, M = 0.1, R_k = 0.5, Pr = 10, Re = 1, Nt = 0.1, Nb = 0.1, Sc = 0.22, Df = 1$ *and* $R = 5$.

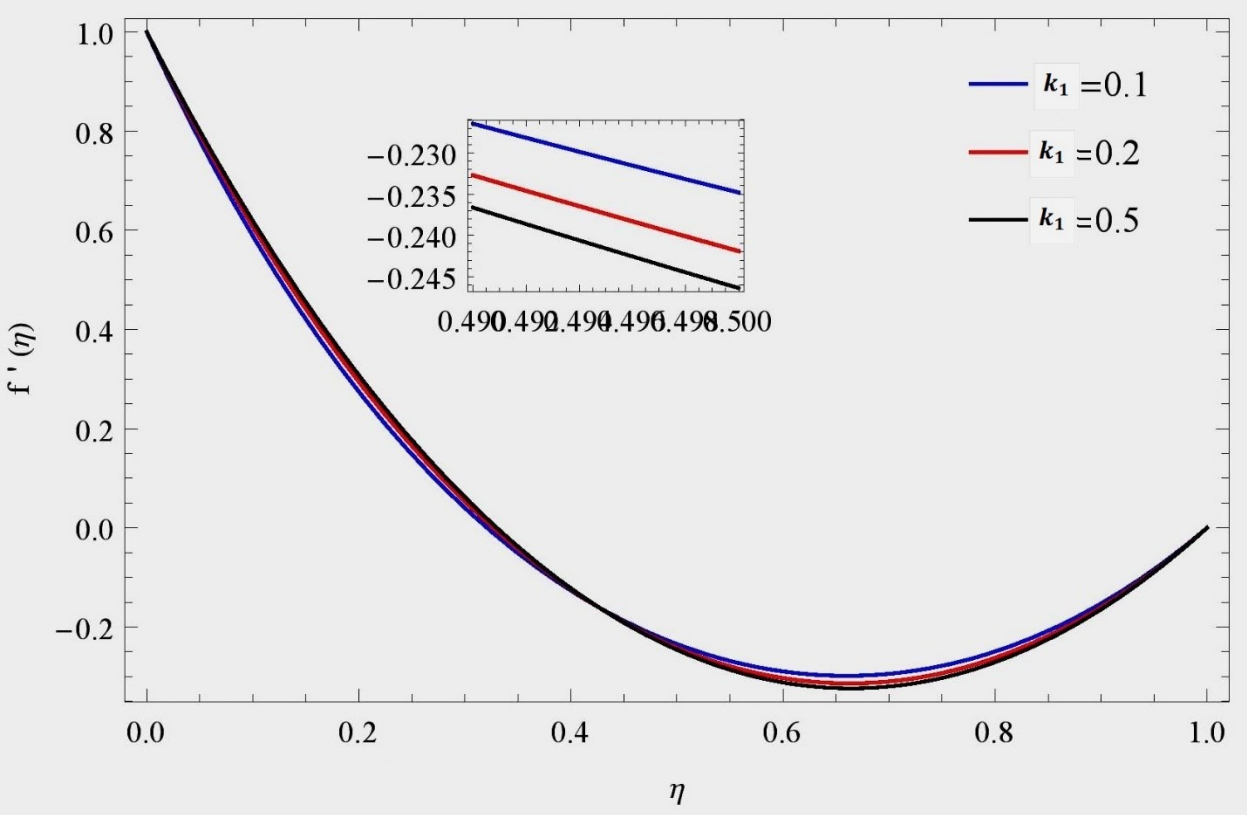

Figure 6.11: $f'(\eta)$ for k_1 at $\gamma = 1, M = 0.1, R_k = 0.5, Pr = 10, Re = 1, Nt = 0.1, Nb = 0.1, Sc = 0.22, Df = 1$ *and* $R = 5$.

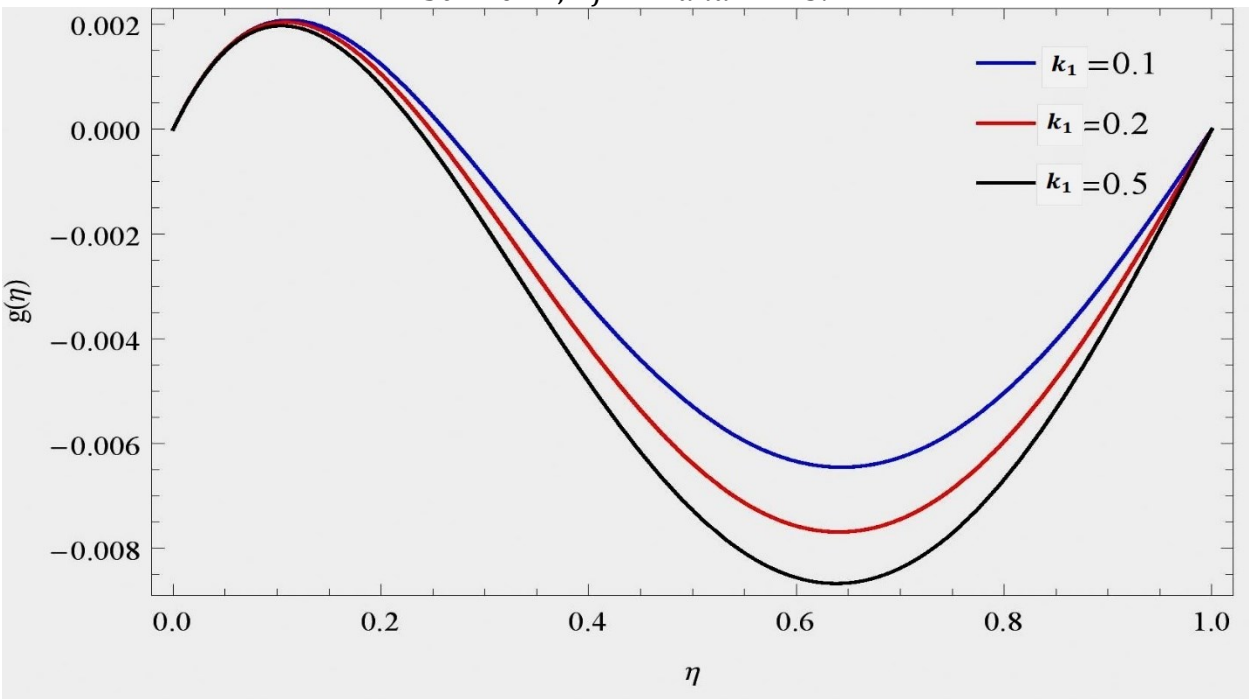

Figure 6.12: $g(\eta)$ for k_1 at $\gamma = 1, M = 0.1, R_k = 0.5, Pr = 10, Re = 1, Nt = 0.1, Nb = 0.1, Sc = 0.22, Df = 1$ *and* $R = 5$.

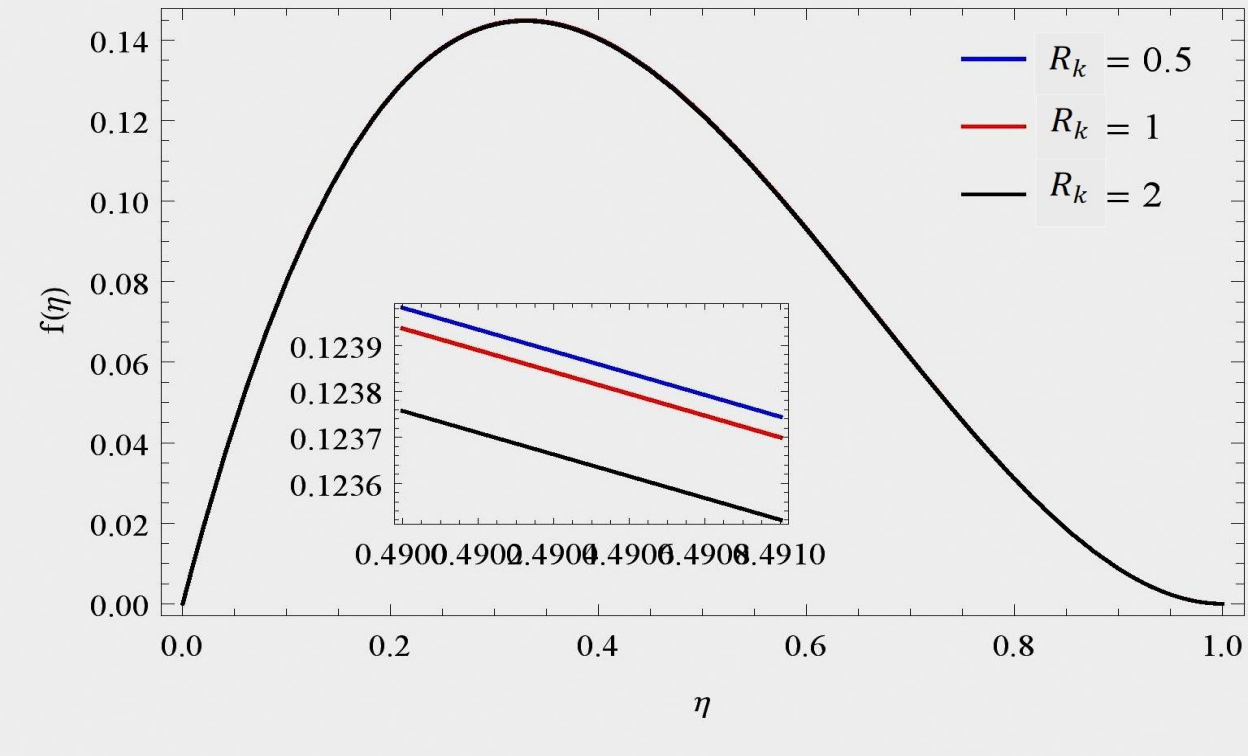

Figure 6.13: $f(\eta)$ for R_k at $\gamma = 1, M = 0.1, k_1 = 0.5, Pr = 10, Re = 1, Nt = 0.1, Nb = 0.1, Sc = 0.22, Df = 1$ *and* $R = 5$.

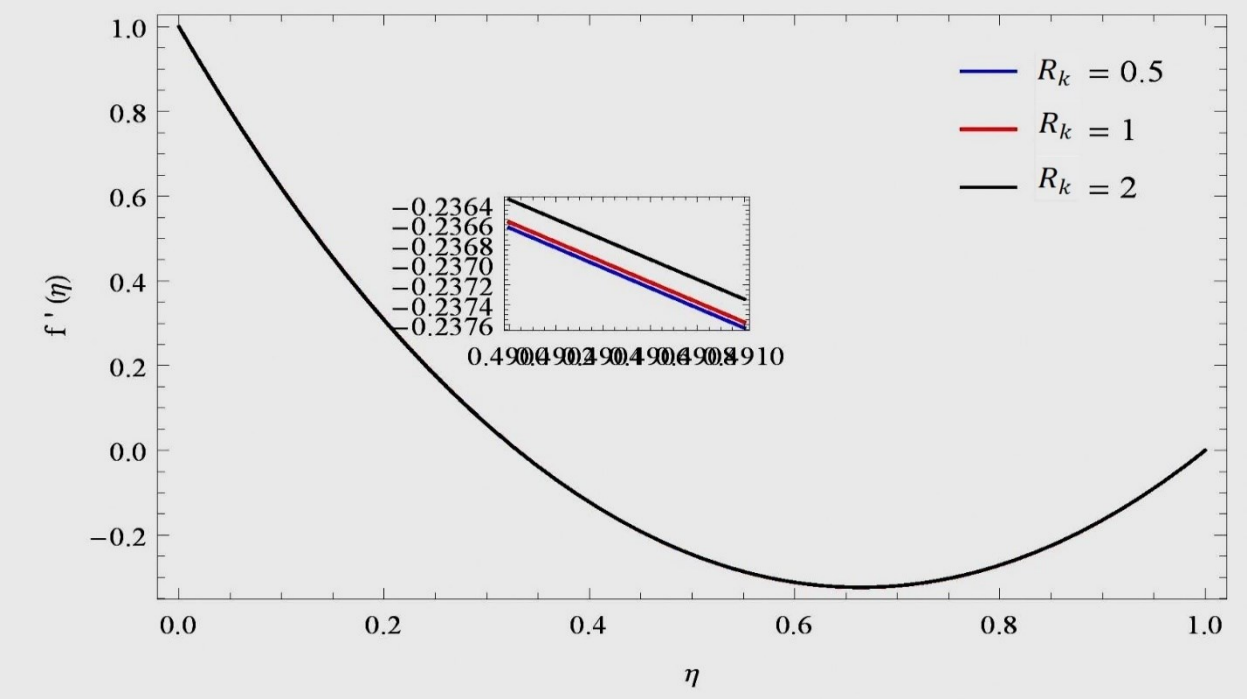

Figure 6.14: $f'(\eta)$ for R_k at $\gamma = 1, M = 0.1, k_1 = 0.5, Pr = 10, Re = 1, Nt = 0.1, Nb = 0.1, Sc = 0.22, Df = 1$ *and* $R = 5$.

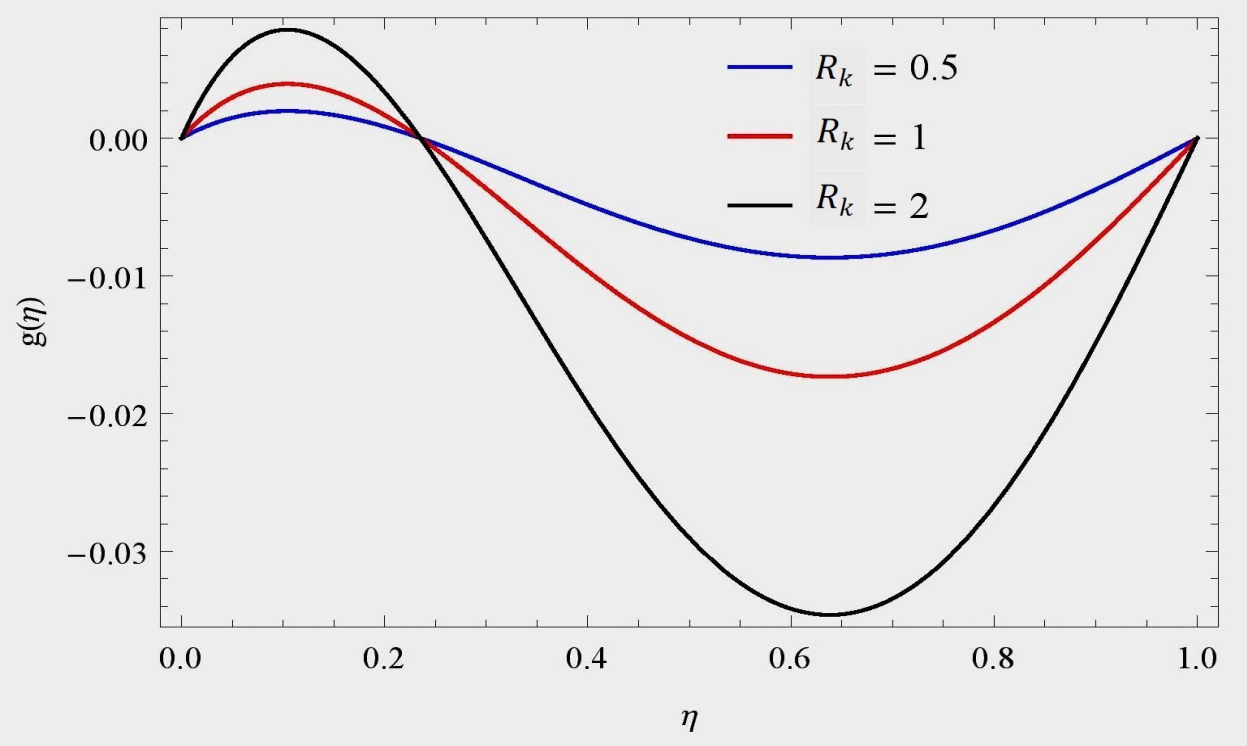

Figure 6.15: $g(\eta)$ for R_k at $\gamma = 1, M = 0.1, k_1 = 0.5, Pr = 10, Re = 1, Nt = 0.1, Nb = 0.1, Sc = 0.22, Df = 1$ *and* $R = 5$.

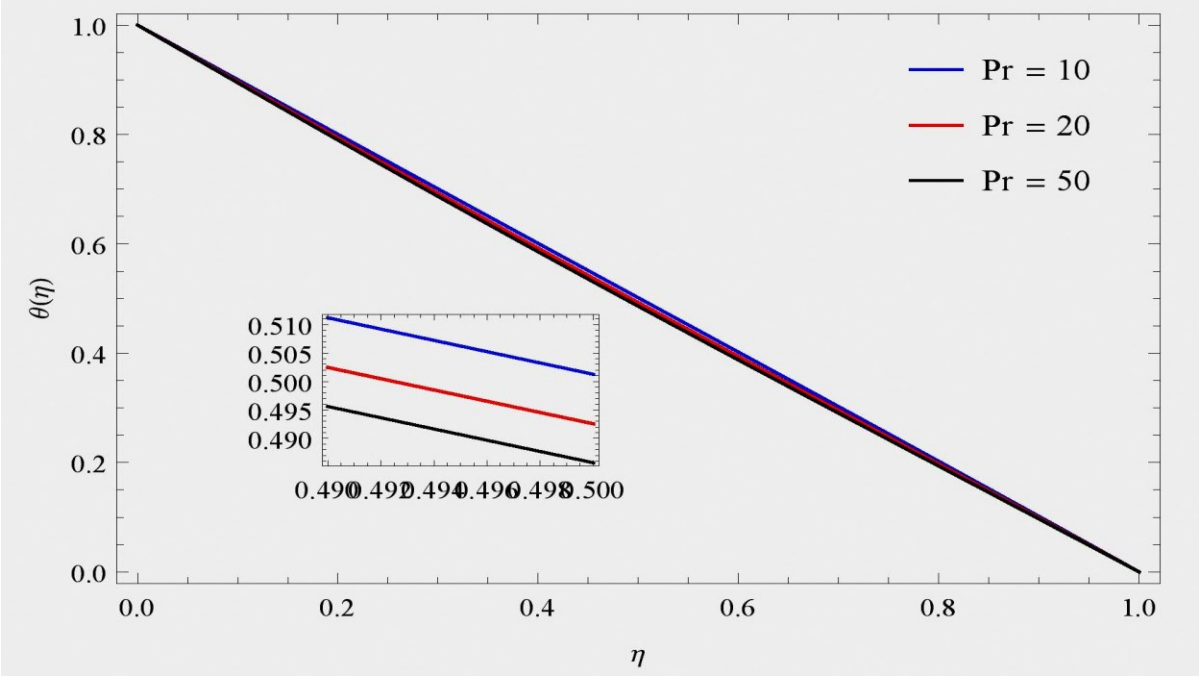

Figure 6.16: $\theta(\eta)$ for Pr at $\gamma = 1, k_1 = 0.5, M = 0.1, Re = 1, Nt = 0.1, Nb = 0.1, Sc = 0.22, Df = 1$ *and* $R = 5$.

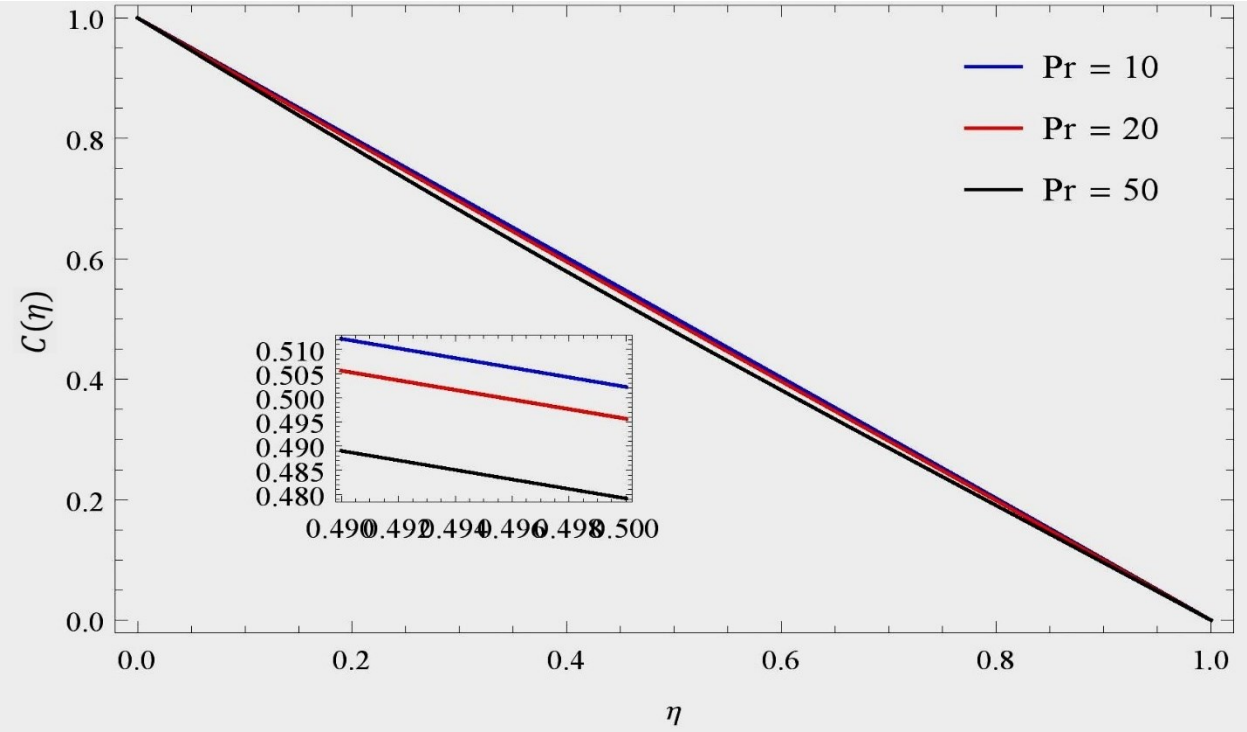

Figure 6.17: $C(\eta)$ for Pr at $\gamma = 1, k_1 = 0.5, M = 0.1, Re = 1, Nt = 0.1, Nb = 0.1,$ $Sc = 0.22, Df = 1$ *and* $R = 5$.

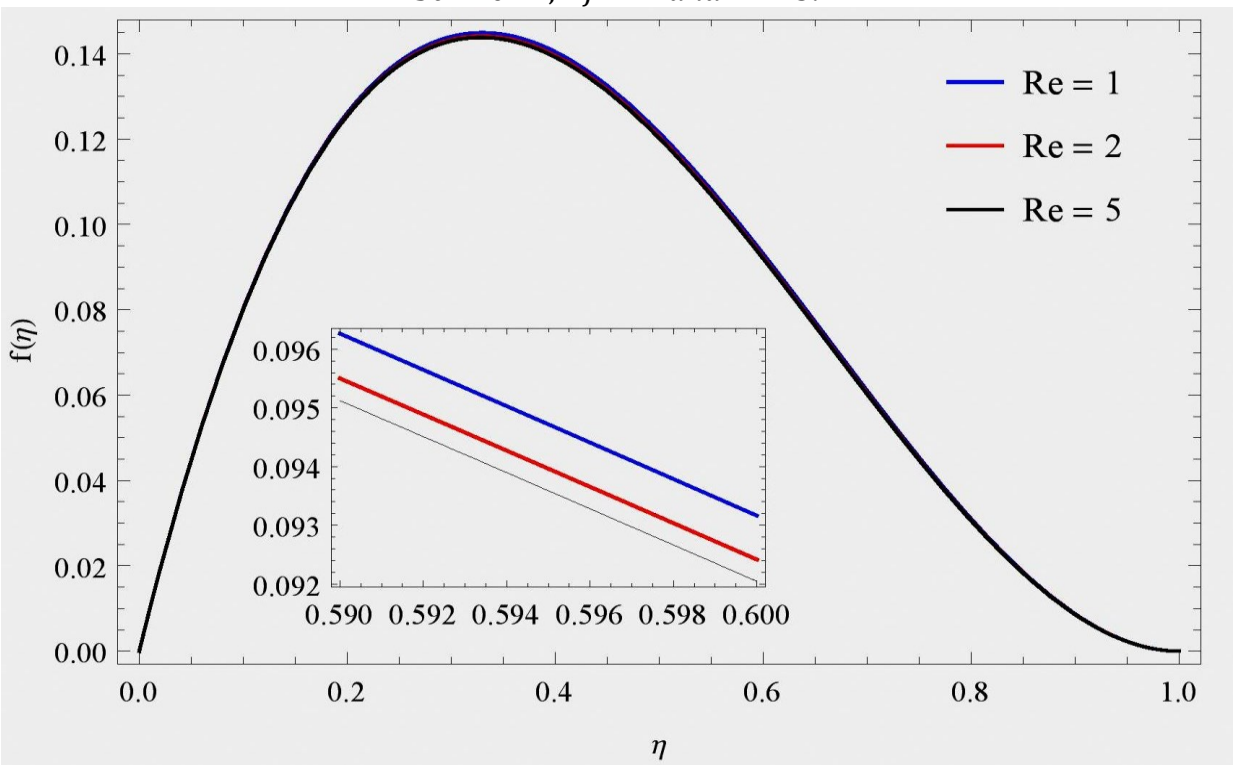

Figure 6.18: $f(\eta)$ for Re at $\gamma = 1, M = 0.1, k_1 = 0.5, Pr = 10, R_k = 0.5, Nt = 0.1,$ $Nb = 0.1, Sc = 0.22, Df = 1$ *and* $R = 5$.

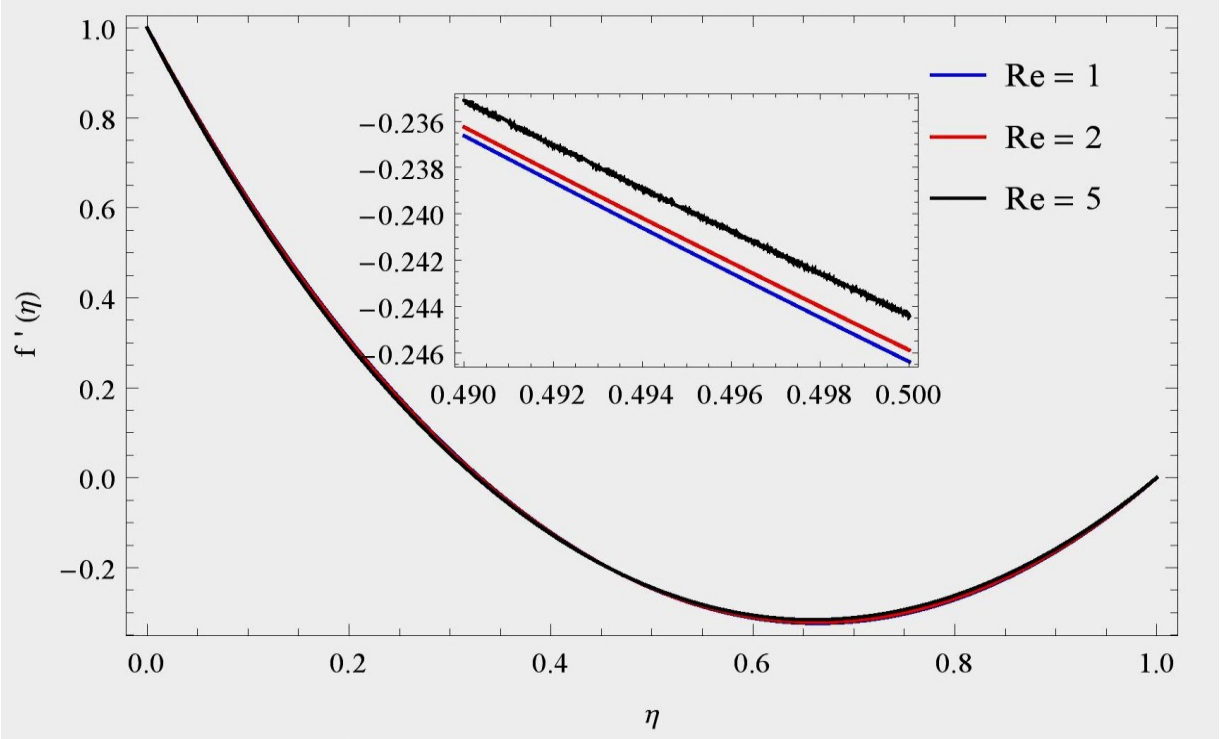

Figure 6.19: $f'(\eta)$ for Re at $\gamma = 1, M = 0.1, k_1 = 0.5, Pr = 10, R_k = 0.5, Nt = 0.1,$ $Nb = 0.1, Sc = 0.22, Df = 1$ and $R = 5$.

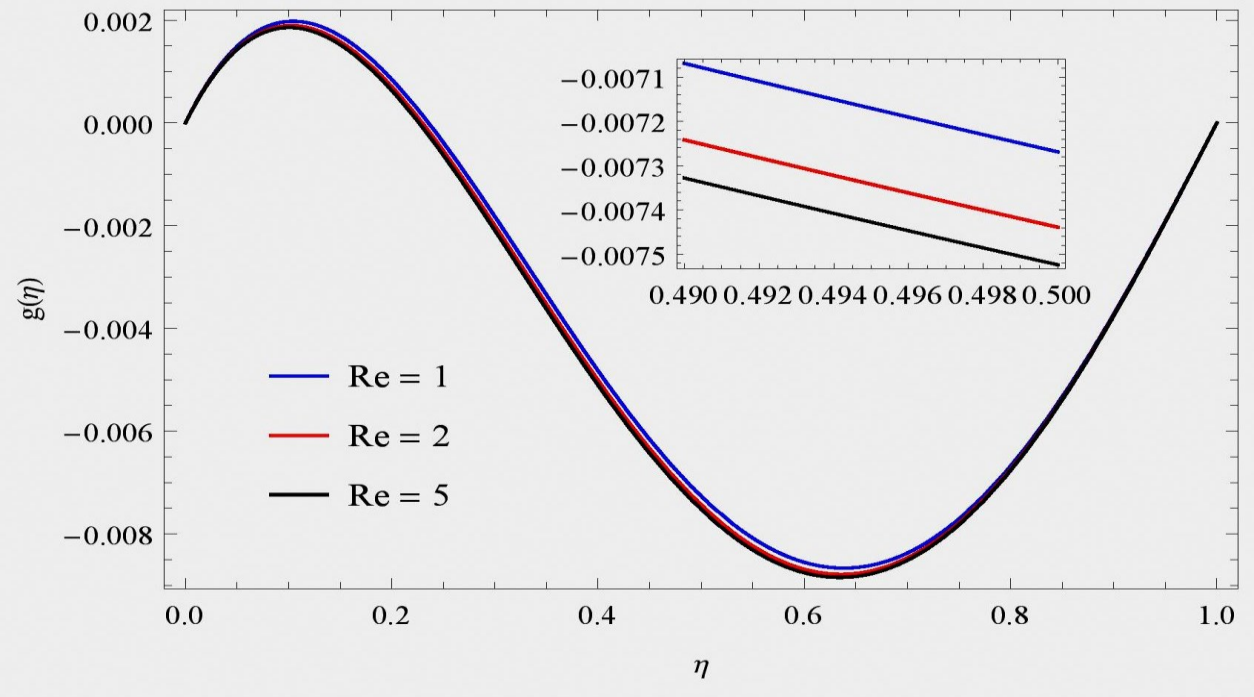

Figure 6.20: $g(\eta)$ for Re at $\gamma = 1, M = 0.1, k_1 = 0.5, Pr = 10, R_k = 0.5, Nt = 0.1,$ $Nb = 0.1, Sc = 0.22, Df = 1$ and $R = 5$.

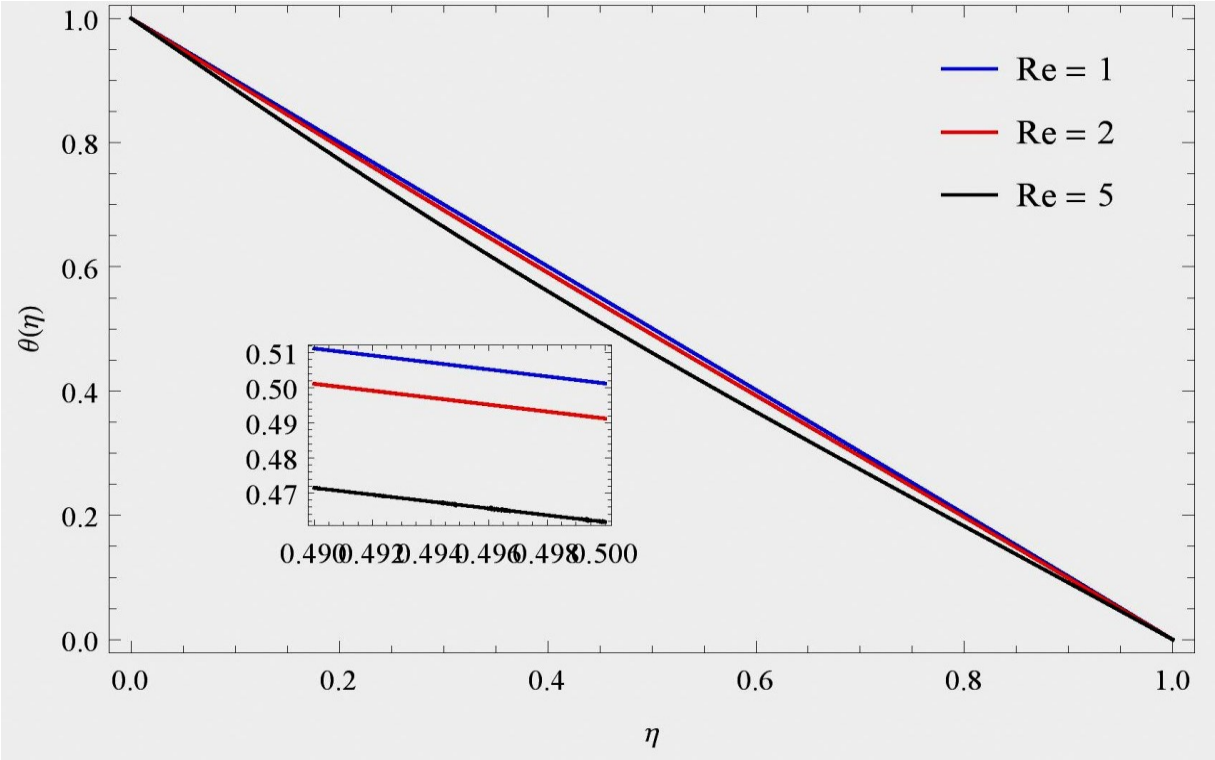

Figure 6.21: $\theta(\eta)$ for Re at $\gamma = 1, M = 0.1, k_1 = 0.5, Pr = 10, Nt = 0.1,$ $Nb = 0.1, Sc = 0.22, Df = 1$ *and* $R = 5$.

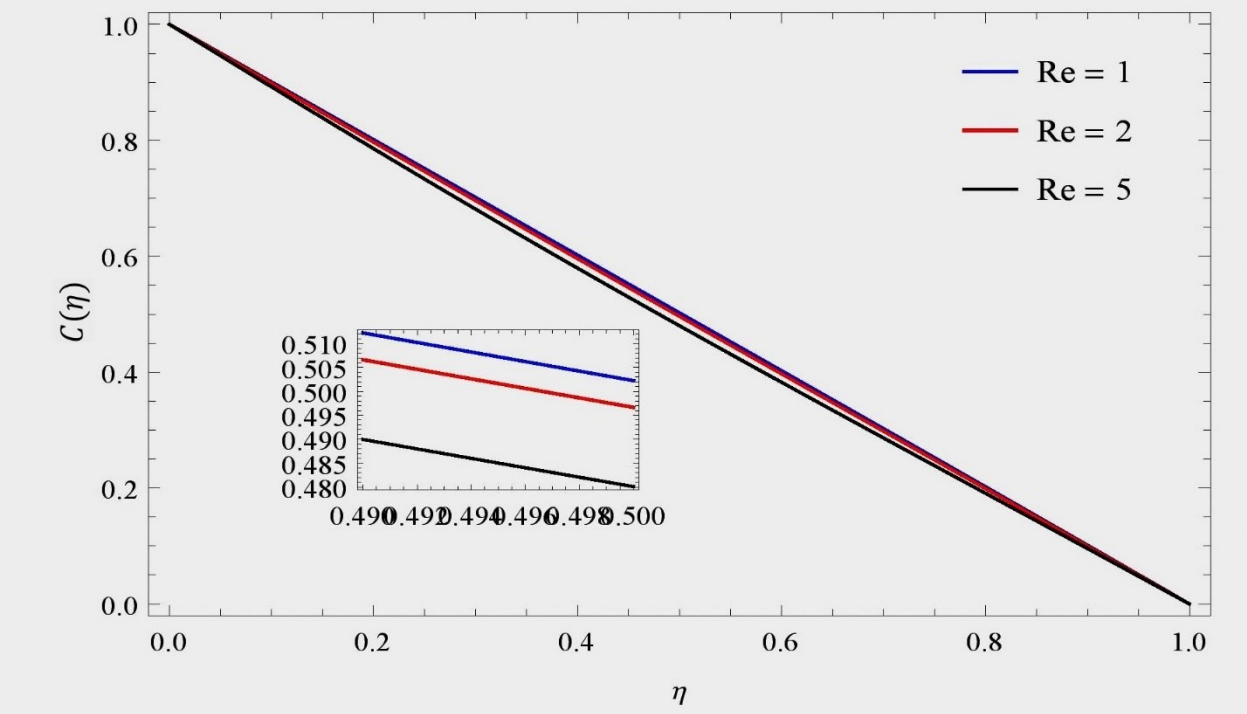

Figure 6.22: $C(\eta)$ for Re at $\gamma = 1, M = 0.1, k_1 = 0.5, Pr = 10,\ Nt = 0.1,$ $Nb = 0.1, Sc = 0.22, Df = 1$ *and* $R = 5$.

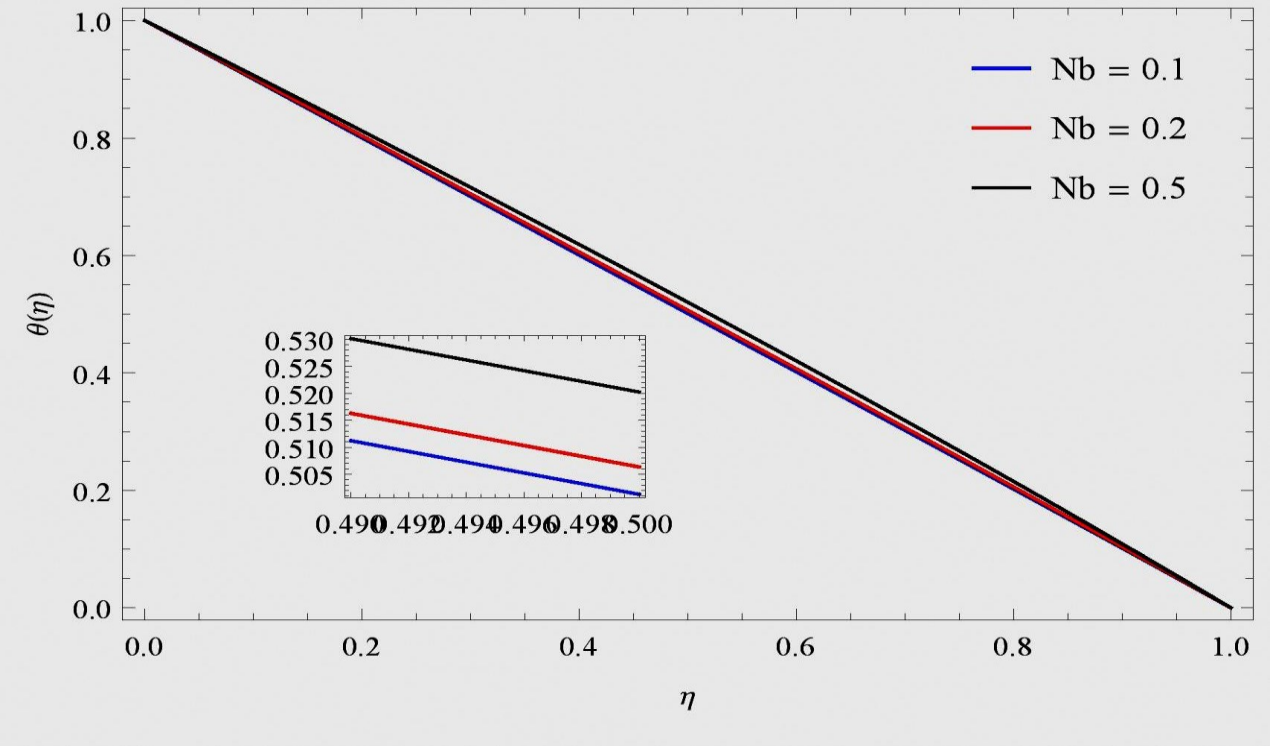

Figure 6.23: $\theta(\eta)$ for Nb at $\gamma = 1, M = 0.1, k_1 = 0.5, Pr = 10,\ Nt = 0.1, Re = 1,$ $Sc = 0.22, Df = 1\ and\ R = 5.$

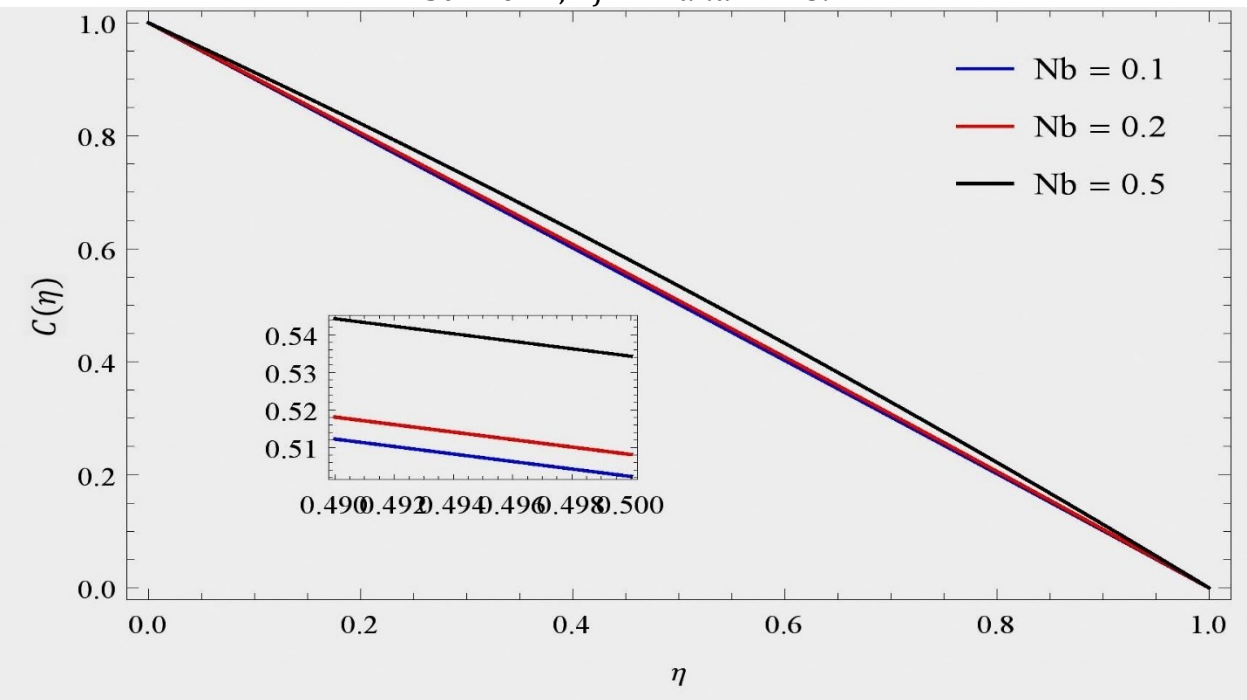

Figure 6.24: $C(\eta)$ for Nb at $\gamma = 1, M = 0.1, k_1 = 0.5, Pr = 10,\ Nt = 0.1, Re = 1,$ $Sc = 0.22, Df = 1\ and\ R = 5.$

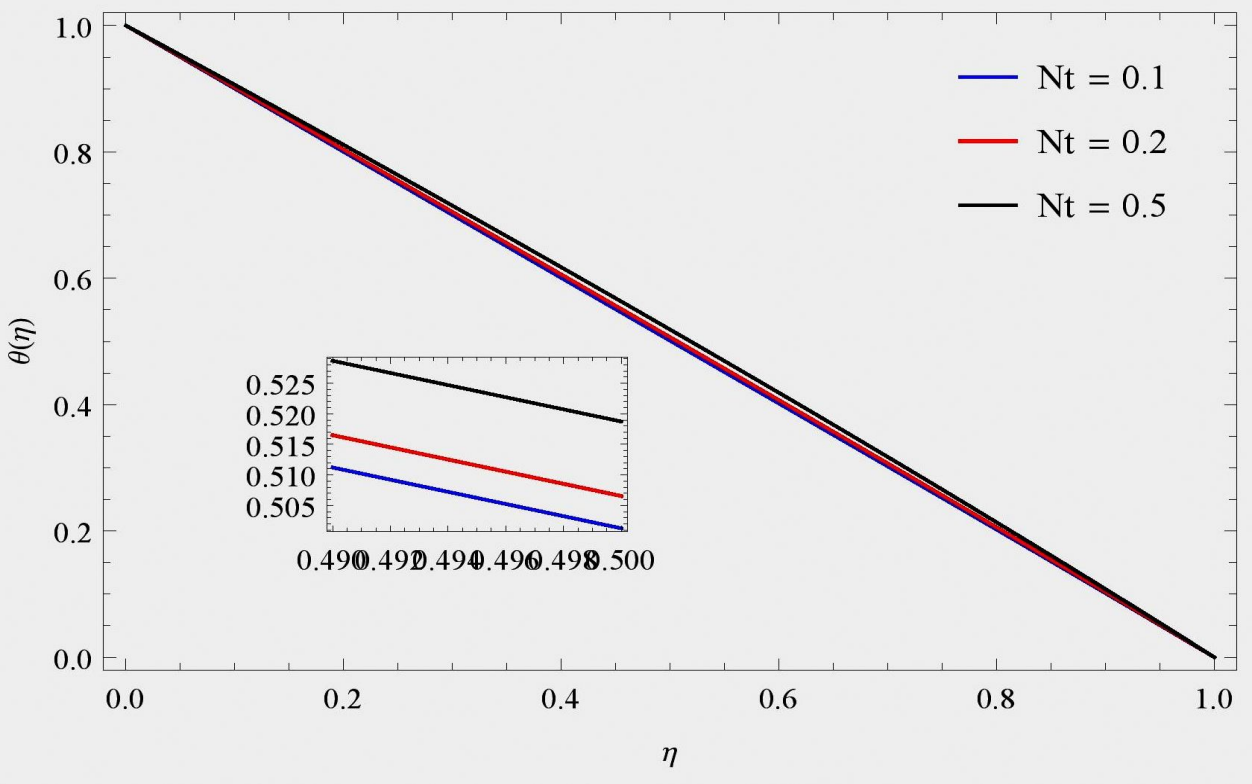

Figure 6.25: $\theta(\eta)$ for Nt at $\gamma = 1, M = 0.1, k_1 = 0.5, Pr = 10, Pr = 10, Re = 1, Nb = 0.1,$ $Sc = 0.22, Df = 1$ and $R = 5$.

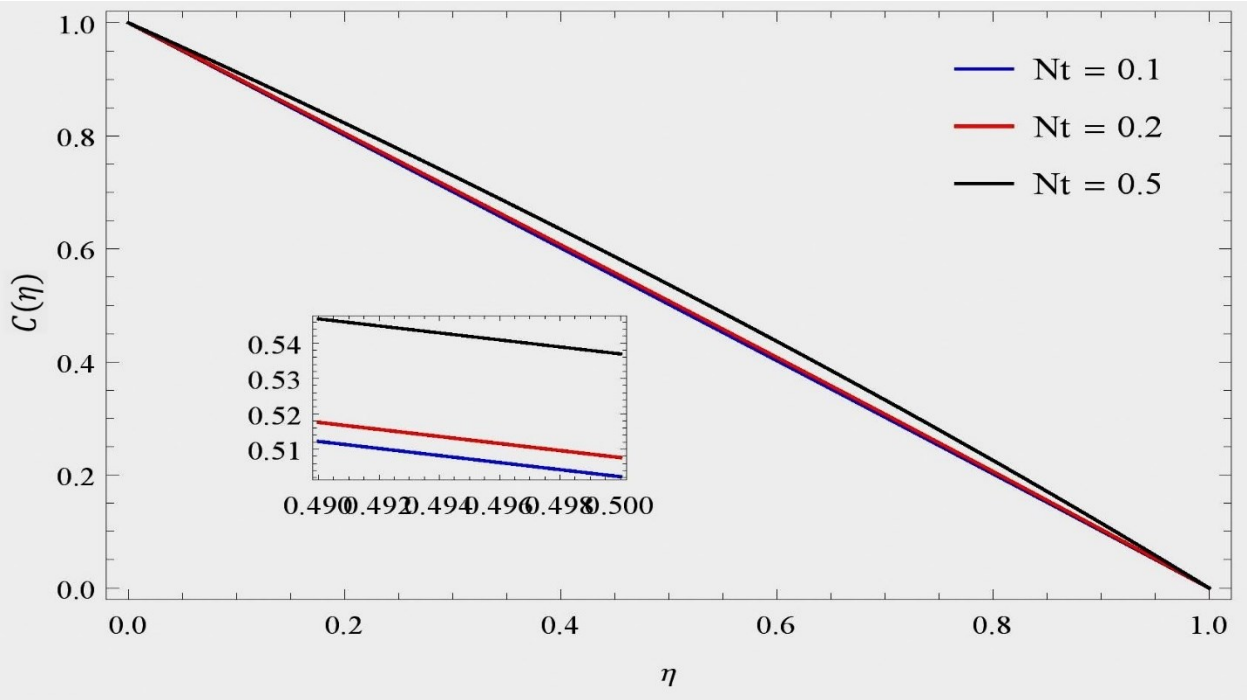

Figure 6.26: $C(\eta)$ for Nt at $\gamma = 1, M = 0.1, k_1 = 0.5, Pr = 10, Pr = 10, Re = 1, Nb = 0.1,$ $Sc = 0.22, Df = 1$ and $R = 5$.

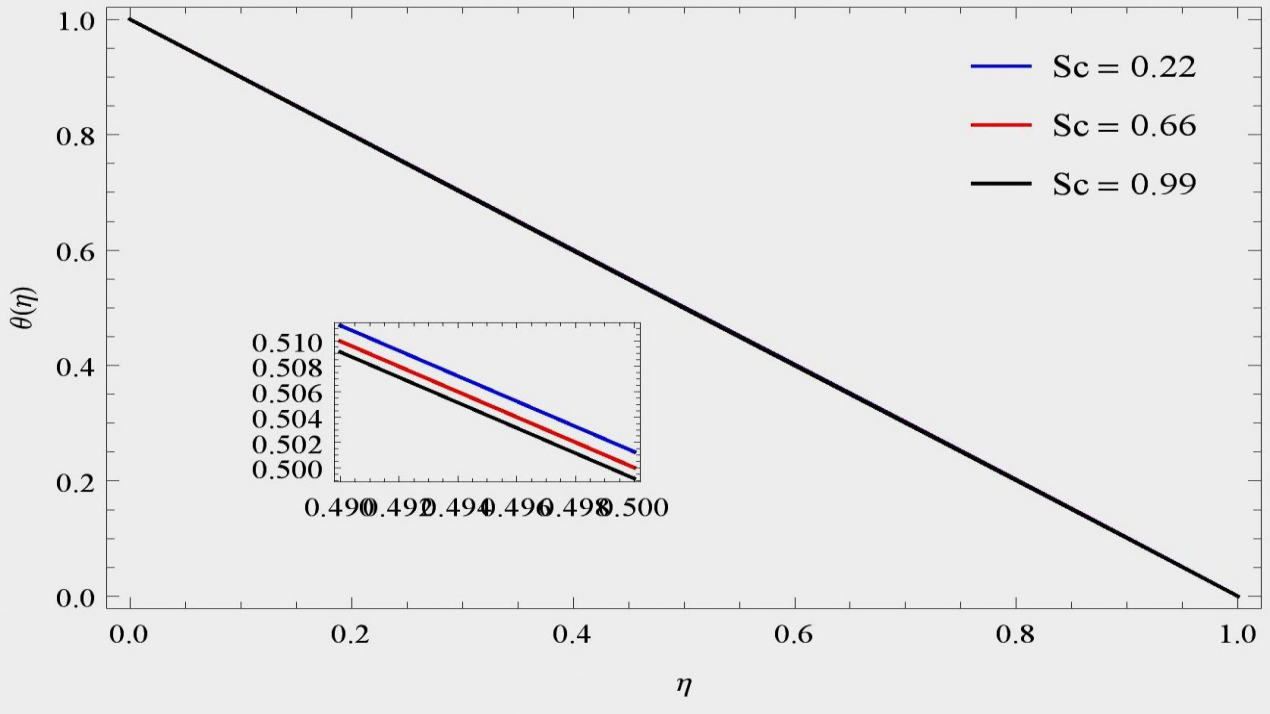

Figure 6.27: $\theta(\eta)$ for Sc at $\gamma = 1, M = 0.1, k_1 = 0.5, Pr = 10,\ Nt = 0.1,$ $Nb = 0.1, Re = 1, Df = 1\ and\ R = 5.$

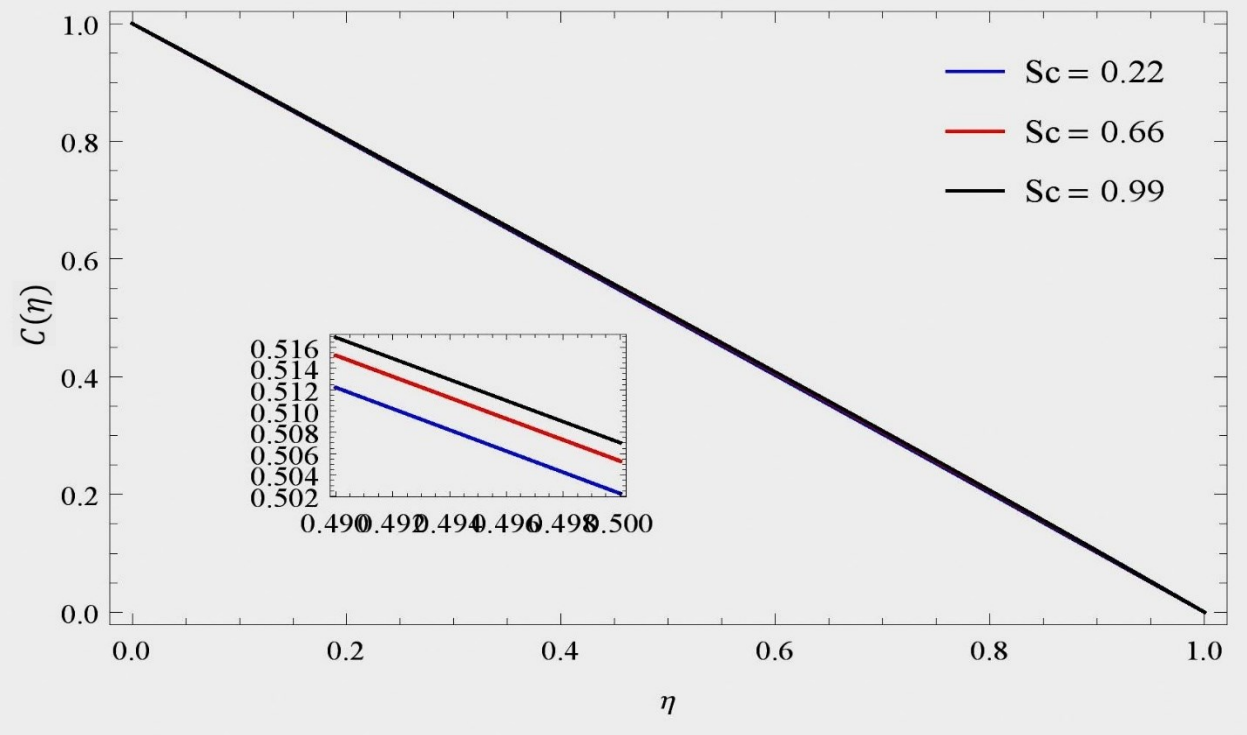

Figure 6.28: $C(\eta)$ for Sc at $\gamma = 1, M = 0.1, k_1 = 0.5, Pr = 10,\ Nt = 0.1,$ $Nb = 0.1, Re = 1, Df = 1\ and\ R = 5.$

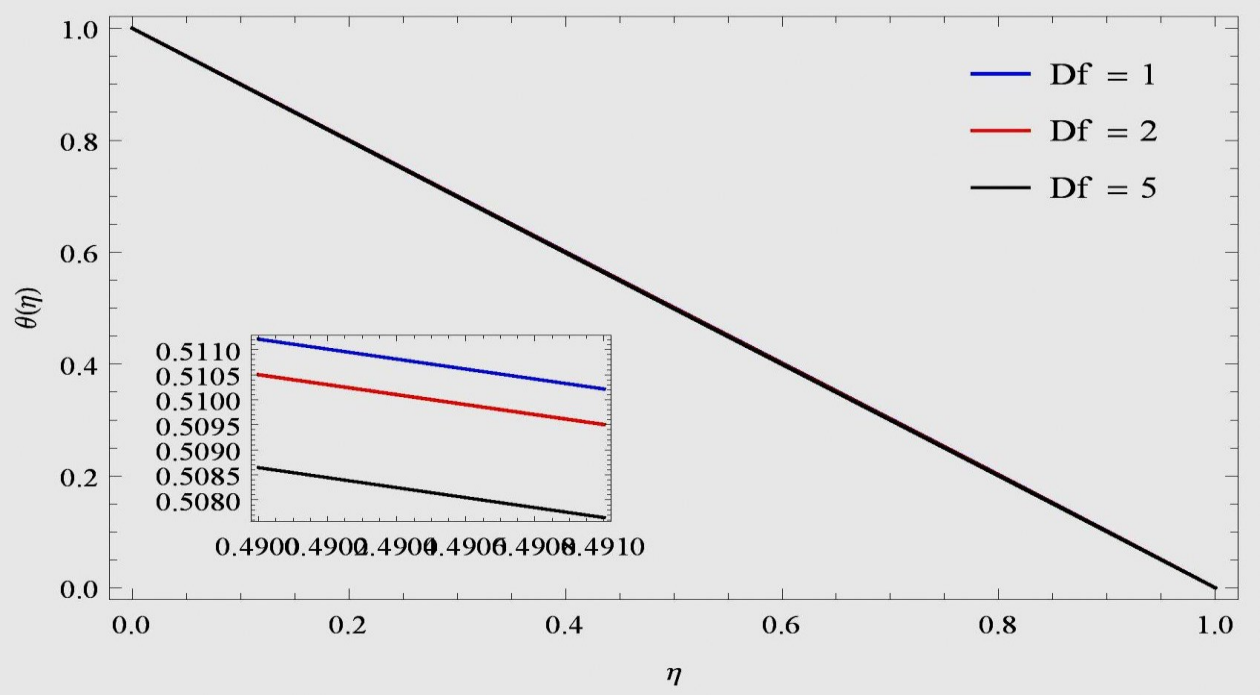

Figure 6.29: $\theta(\eta)$ for Df at $\gamma = 1, M = 0.1, k_1 = 0.5, Pr = 10,\ Nt = 0.1,$ $Nb = 0.1, Sc = 0.22, Re = 1\ and\ R = 5.$

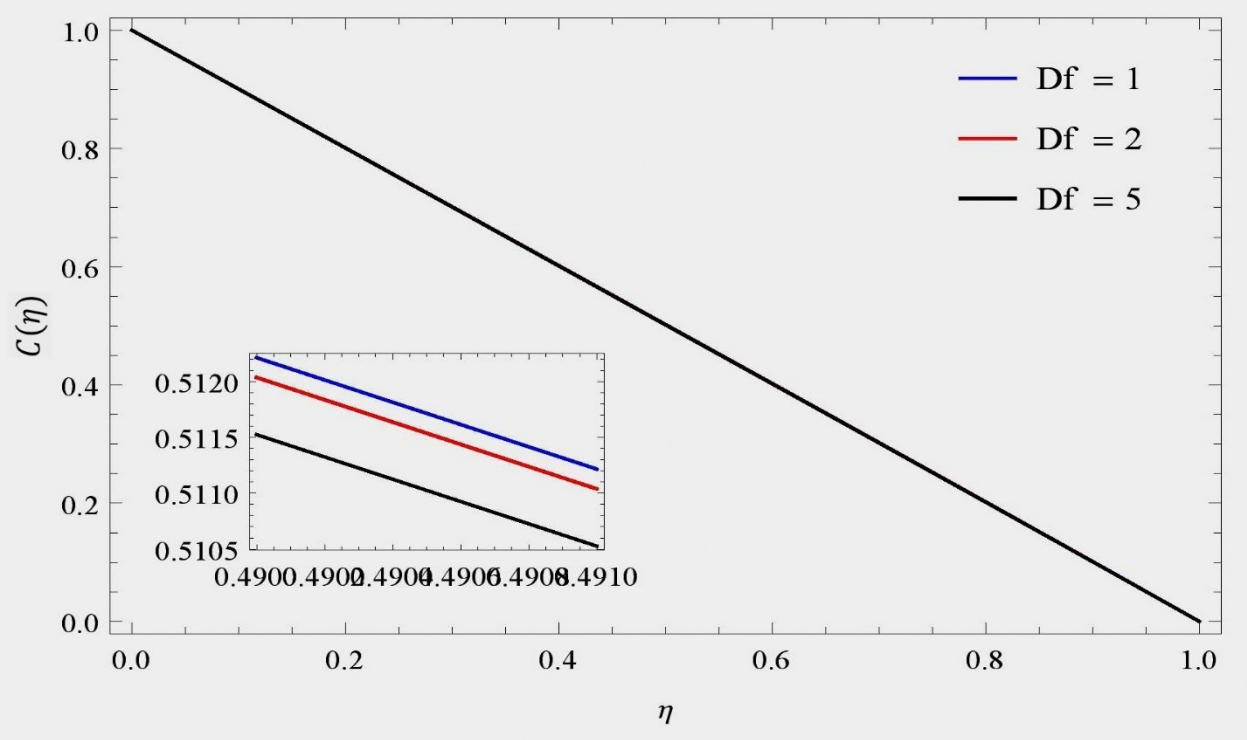

Figure 6.30: $C(\eta)$ for Df at $\gamma = 1, M = 0.1, k_1 = 0.5, Pr = 10,\ Nt = 0.1,$ $Nb = 0.1, Sc = 0.22, Re = 1\ and\ R = 5.$

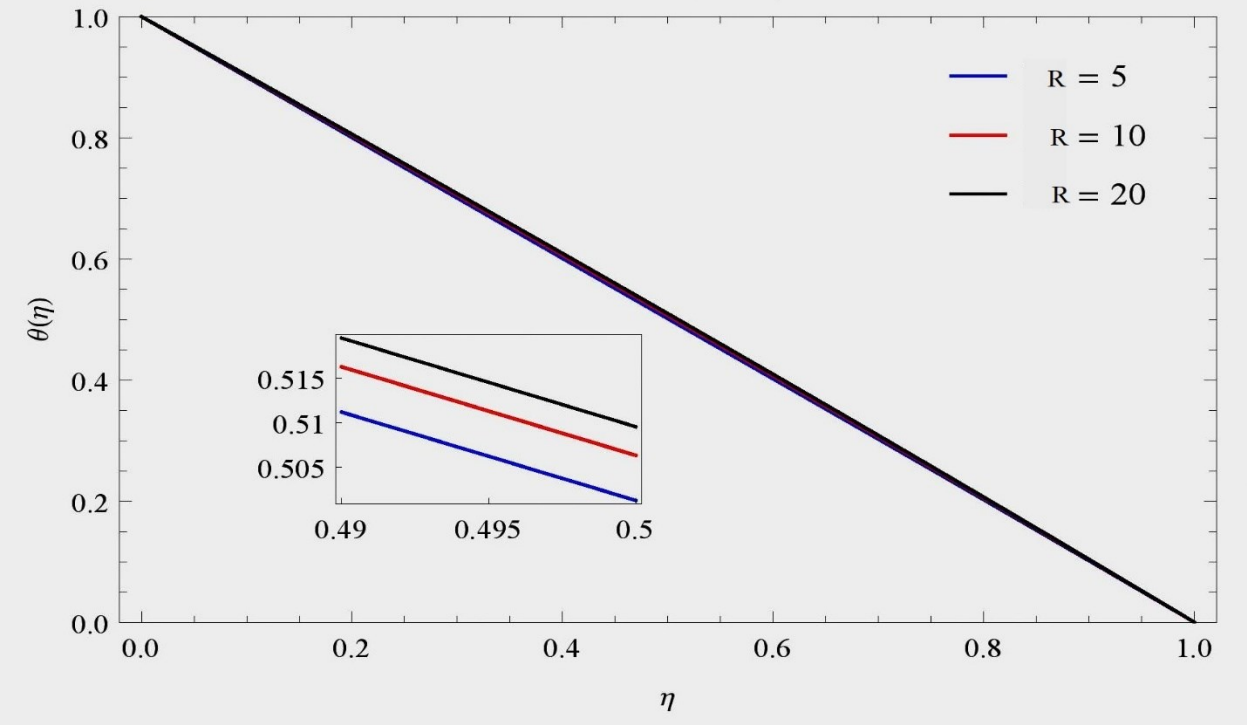

Figure 6.31: $\theta(\eta)$ for R at $\gamma = 1, M = 0.1, k_1 = 0.5, Pr = 10, Pr = 10, Nt = 0.1, Nb = 0.1, Sc = 0.22, Re = 1$ *and* $Df = 1$.

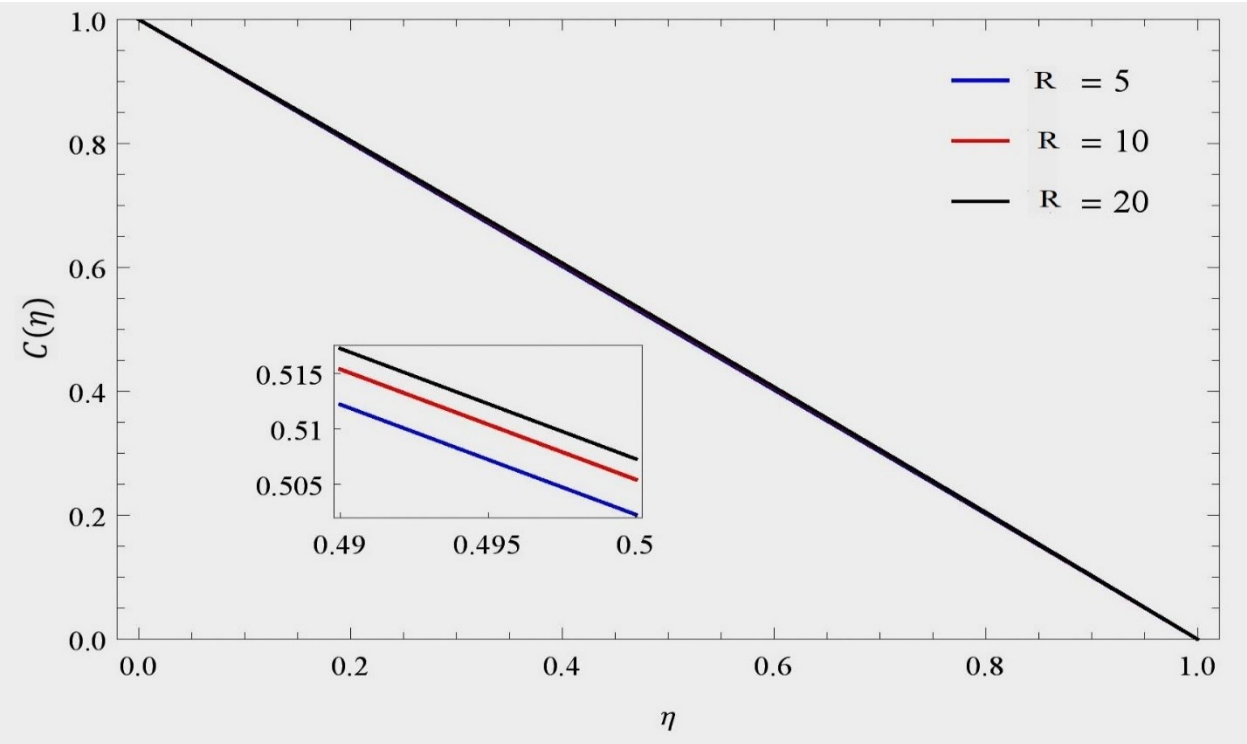

Figure 6.32: $C(\eta)$ for R at $\gamma = 1, M = 0.1, k_1 = 0.5, Pr = 10, Pr = 10, Nt = 0.1, Nb = 0.1, Sc = 0.22, Re = 1$ *and* $Df = 1$.

Figures 6.16 – 6.17 depict fall temperature and concentration profiles with higher values of Pr. Actually, increment in Pr leads to decrement in thermal conductivity of the fluid which deduce to decrement in boundary layer thickness. Figures 6.18 – 6.22 gives effect of Re on velocity, temperature and concentration. One can observe that higher values of Re tends to improve velocity in y direction while reduce in x and z direction. Also, increment in Re will reduce temperature and concentration. Figures 6.23 – 6.24 reflects effects of Nb on temperature and concentration profiles. It is noted that both have positive changes with increase in Nb. Figures 6.25 – 6.26 describes increase in thermophoresis parameter Nt results increase in temperature and concentration profiles. Figures 6.27 – 6.28 exhibit temperature and concentration profiles for Schmidt number Sc. It can be noted that temperature falls with increase in Sc whereas concentration rises with rise of Sc. Figures 6.29 – 6.30 reflect dufour effect Df on temperature and concentration. It can be observed that both have negative tendency with augmentation in Df. Figures 6.31 – 6.32 illustrate that radiation have positive tendency on temperature as well as concentration.

6.6 Conclusion:

From the observations of all results, the following can be concluded.

- Fluid velocity decreases with increase in M, Kr and Re.
- Fluid velocity intensifies with k_1.
- Fluid temperature can be raised by increment in either R, R_k, Nt or Nb.
- Fluid temperature has retarding effect with growing values of Re, Df or Pr.
- Concentration can be increased by increasing values of Nt, Sc or Nb, and reverse is for R.